THE HONG KONG UNIVERSITY OF SCIENCE AND TECHNOLOGY

Final Report

for

Provision of Service for Fine Particulate Matter ($PM_{2.5}$) Sample Chemical Analysis

(Tender Ref. 11-03973)

Prepared by:

Prof. Jian Zhen Yu

Dr. X. H. Hilda Huang

Ms. Wai Man Ng

Environmental Central Facility

The Hong Kong University of Science & Technology

Clear Water Bay, Kowloon, Hong Kong

Presented to:

Environmental Protection Department

The Government of the Hong Kong Special Administrative Region

June 2013

Table of Contents

List of Tables

List of Figures

1. Introduction

1.1 Study Objectives

The Environmental Central Facility (ENVF) at the Hong Kong University of Science and Technology (HKUST) assisted the Hong Kong Environmental Protection Department (HKEPD) in the analysis of $PM_{2.5}$ samples acquired over the course from February 2012 to December 2012. The objectives of this study were to:

- Determine the organic and inorganic composition of $PM_{2.5}$ and how it differs by season and proximity to different types of emission sources.
- Based on the ambient concentrations of certain tracer compounds, determine the contributions of different sources to $PM_{2.5}$ in Hong Kong.
- Investigate and understand the influences of meteorological/atmospheric conditions on $PM_{2.5}$ episodic events in Hong Kong.
- Establish inter-annual variability of $PM_{2.5}$ concentration and chemical composition in Hong Kong urban and rural areas.

1.2 Background

The Hong Kong government proposed new Air Quality Objectives (AQOs) in January 2012. The proposed AQOs for $PM_{2.5}$ were a 24-hour average of 75 $\mu g/m^3$ and a yearly average of 35 $\mu g/m^3$. The proposed AQOs are now in the legislative process and are expected to take effect in 2014.

This report documents the $PM_{2.5}$ measurements and data validation for an eleven-month study from February 2012 to December 2012 in order to get a better understanding on the nature and contribution of sources for air pollution trend analysis. The data will be analyzed to characterize the composition and temporal and spatial variations of $PM_{2.5}$ concentrations. The main objectives of the study include: 1) establish the trend of $PM_{2.5}$ concentration and chemical composition by comparing previous 12-month $PM_{2.5}$ studies during 2000 and 2001, 2004 and 2005, 2008 and 2009, and the whole year of 2011; 2) explore the contribution of different emission sources to the $PM_{2.5}$ loading in Hong Kong, and 3) investigate the hypotheses regarding the formation of $PM_{2.5}$ episodes.

1.3 Technical Approach

During the sampling period from February 2012 to December 2012, 24-hour $PM_{2.5}$ mass measurements were acquired once every six days from the roadside-source-dominated Mong Kok (MK) Air Quality Monitoring Site (AQMS), the urban Central/Western (CW) and Tsuen Wan (TW) AQMSs, the new town Tung Chung (TC) and Yuen Long (YL) AQMSs, and the suburban Clear Water Bay (WB) Air Quality Research Site (AQRS) which is located on the campus of the Hong Kong University of Science and Technology. Three Partisol particle samplers (Rupprecht & Patachnick, Model 2025, Albany, NY) were used at MK, CW, WB, and TC sites while two Partisol samplers were placed at TW and YL sites to obtain $PM_{2.5}$ samples on both Teflon-membrane and QMA 47-mm filters. All sampled Teflon-membrane and QMA filters were analyzed for mass by gravimetry by HKEPD's contractor and then subjected to a suite of chemical analyses, including 1) measurements of elements for atomic number

ranging from 11 (Sodium) to 92 (Uranium) using ED-XRF Spectroscopy; 2) carbon analysis using a Thermal/Optical Carbon Analyzer by both Thermal Optical Transmittance (TOT) and Thermal Optical Reflectance (TOR) methods; 3) Ionic measurements using Ion Chromatography.

2. Sampling Network

2.1 Ambient $PM_{2.5}$ Monitoring Network

24-hour $PM_{2.5}$ filter samples were taken at five air quality monitoring sites (AQMSs) and one air quality research supersite (AQRS) in Hong Kong once every six days from February 2012 to December 2012. The six sampling sites are shown in Figure 1, representing roadside (MK), urban (CW and TW), new town (TC and YL), and suburban (WB) areas. The names, codes, locations, and descriptions of individual sites are listed in Table 1.

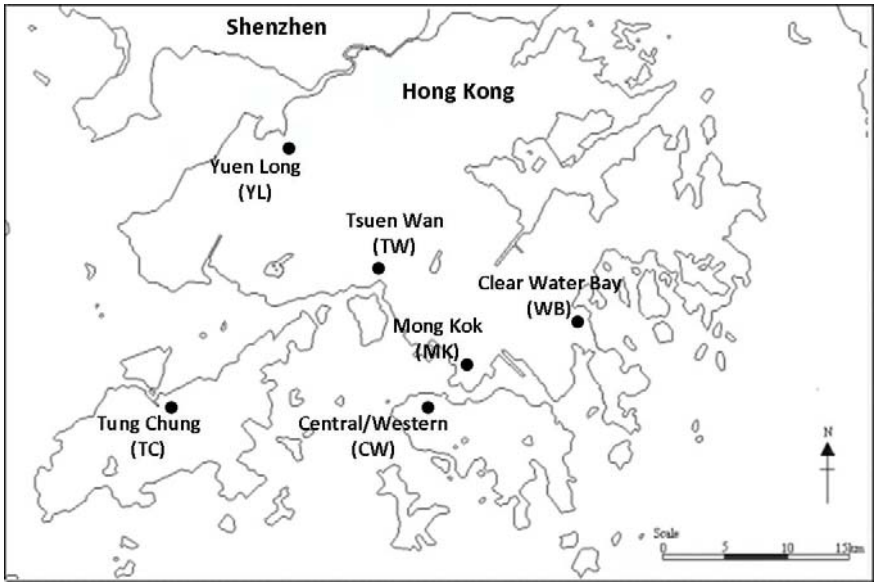

Figure 1. $PM_{2.5}$ monitoring sites in Hong Kong for characterization study.

Table 1. Descriptions of monitoring sites

Site Name	Site Code	Site Location	Site Description
Mong Kok	MK	Junction of Lai Chi Kok Road and Nathan Road, Kowloon	Urban roadside in mixed residential/commercial area with heavy traffic and surrounded by many tall buildings
Central/Western	CW	Rooftop of Sai Ying Pun Community Center, No. 2 High Street, Sai Ying Pun, Hong Kong	Urban, densely populated, residential site with mixed commercial development
Clear Water Bay	WB	Rooftop of a pump house next to Coastal Marine Lab, HKUST Campus, Clear Water Bay	Clean rural area with little residential and commercial development on the east coast of Sai Kung
Tung Chung	TC	Rooftop of Tung Chung Health Center, No. 6 Fu Tung Street, Lantau Island	Residential town, within 5 km southeast of HK International Airport

Site Name	Site Code	Site Location	Site Description
Tsuen Wan	TW	Rooftop of Princess Alexandra Community Center, 60 Tai Ho Road, New Territories	Urban, densely populated, residential site with mixed commercial and industrial developments. Located northwest of the MK site
Yuen Long	YL	Rooftop of Yuen Long District Branch Office Building, 269 Castle Peak Road, New Territories	Residential town, about 15 km southwest of Shenzhen

2.2 Ambient $PM_{2.5}$ Measurements

A total of 16 Partisol samplers were employed to obtain $PM_{2.5}$ samples around Hong Kong. The detailed arrangement of the samplers is described in Table 2.

Table 2. Arrangement of the Partisol samplers in monitoring sites.

Location	No. of Samplers	Collocated Samples
MK AQMS	3	Teflon Filters
CW AQMS	3	Teflon Filters
WB AQRS	3	QMA Filters
TC AQMS	3	QMA Filters
TW AQMS	2	
YL AQMS	2	

Each Partisol sampler was equipped with an Andersen $PM_{2.5}$ inlet with Very Sharp Cut Cyclone (VSCC). The samplings were conducted at a flow rate of 16.7 L/min. At this flow rate, a nominal volume of approx. 24.0 m^3 of ambient air would be sampled over a 24-hour period. The Partisol samplers were configured to take either a Teflon-membrane filter or a QMA filter. For this study, the following filters were chosen: 1) Whatman (Clifton, NJ, USA), PM2.5 membrane, PTFE, 46.2 mm with support ring (#7592204); and 2) Pall Life Sciences (Ann Arbor, MI, USA), 2500QAT-UP, 47 mm, Tissuquartz^{TM} filters (#7202).

The Partisol samplers were operated and maintained by HKEPD's contractor, AECOM with support from the Hong Kong Polytechnic University (PolyU) throughout the study period. The PolyU team was responsible for pre- and post-sampling procedures required for quality assurance and sample preservation. PolyU team was also responsible for the mass measurement and analysis on both filter types before and after sampling.

The collected Teflon-membrane filters were used for mass analysis by gravimetry and elemental analysis (for more than 40 elements with atomic number ranging from 11 to 92) by X-Ray Fluorescence [*Watson et al.*, 1999]. The collected QMA filters were analyzed for mass by gravimetry, for carbon content by multiple thermal evolution methods, and for chloride (Cl^-), nitrate (NO_3^-), sulfate (SO_4^{2-}), water-soluble sodium (Na^+), ammonium (NH_4^+), and water-soluble potassium (K^+) by ion chromatography.

A major uncertainty in determining carbon concentrations lies in the differentiation of organic and elemental carbon during analysis. EC has been defined as the carbon that evolves after the detected optical signal attains the value it had prior to commencement of heating and the rest of the carbon is considered to be OC [*Chow et al.*, 1993; *Birch and Cary*, 1996]. The split of OC and EC in the thermal analysis depends on several parameters including temperature setpoints, temperature ramping rates, residence time at each setpoint, combustion atmospheres, and optical signal used. Heating in an inert atmosphere causes certain OC to pyrolyze or char, inflating the EC in the sample. The extent of pyrolysis is affected by different thermal/temperature protocols. A laser is used to overcome this problem by monitoring changes in filter darkness during the thermal evolution process by detecting either filter transmittance (thermal/optical transmittance [TOT] method) or reflectance (thermal/optical reflectance [TOR] method). However, this introduces another problem of inner/near-surface filter pyrolysis. It is found that pyrolysis occurs both within filter and on the filter surface. TOT method measures light transmittance which goes through the filter and is more likely influenced by the inner filter char while TOR method is more influenced by the charring of near-surface deposit.

In this study, two analytical protocols - National Institute of Occupational Safety and Health (NIOSH 5040) protocol coupled with TOT method for charring correction, and the Interagency Monitoring of Protected Visual Environments (IMPROVE) protocol coupled with TOR method for charring correction are employed to analyze the QMA filters. Table 3 shows the temperature programs of the NIOSH and IMPROVE protocols. Results obtained with the two protocols are compared and evaluated in Section 3.3.4.

Table 3. Temperature programs of the IMPROVE and the NIOSH protocols.

Methods' carrier gas	Carbon fraction	NIOSH_TOT temp, time	IMPROVE_TOR* temp, time
He purge		25 °C, 10 s	25 °C, 10 s
He-1	OC1	310 °C, 80 s	120 °C, 180 s
He-2	OC2	475 °C, 60 s	250 °C, 180 s
He-3	OC3	615 °C, 60 s	450 °C, 180 s
He-4	OC4	870 °C, 90 s	550 °C, 180 s
He-5		Cool oven	-
O_2 / He-1	EC1	550 °C, 45 s	550 °C, 240 s
O_2 / He-2	EC2	625 °C, 45 s	700 °C, 210 s
O_2 / He-3	EC3	700 °C, 45 s	850 °C, 210 s
O_2 / He-4	EC4	775 °C, 45 s	
O_2 / He-5	EC5	850 °C, 45 s	
O_2 / He-6	EC6	870 °C, 45 s	

* The IMPROVE temperature program was used for measurements reported in this work. Another related temperature protocol, termed IMPROVE_A, is typically adopted on DRI Model 2001 carbon analyzers. The IMPROVE_A temperature protocol defines temperature plateaus of 140 °C for OC1, 280 °C for OC2, 480 °C for OC3, and 580 °C for OC4 in a helium (He) carrier gas and 580 °C for EC1, 740 °C for EC2, and 840 °C for EC3 in a 98% He/2% oxygen (O_2) carrier gas [*Chow et al.*, 2007]. These temperatures used with the new hardware in DRI Model 2001 better match the sample temperatures experienced in the analysis using the IMPROVE protocol on the previous models of DRI analyzers.

2.3 Sample Delivery and Filter Conditions

The filter samples were delivered to the HKUST project team by AECOM on August 24, 28, September 20, October 30 and November 15, 2012, and January 3 and 23, 2013. A total of 976 samples including 488 pieces of Teflon filters and 488 pieces of QMA filters were received. The sampling dates on which the samples were collected were summarized in Table 4. On 30 sampling days, $PM_{2.5}$ samples were collected at all of the sampling sites. These days are shaded in grey color in Table 4.

Table 4. Valid sampling dates for the $PM_{2.5}$ samples (Tender Ref. 11-03973).

Sampling Dates	Sampling Sites with Sample Collection
120211	MK, CW, WB, TC, TW
120215	YL
120217	MK, WB, TC, TW, YL
120229	CW
120306	MK, CW, WB, TC, YL
120306 BLANK	MK, CW, WB, TC, TW, YL
120308	TW
120312	MK, CW, WB, TC, TW
120316	MK, CW, WB, TC, TW
120318	MK, CW, WB, TC, TW
120322	YL
120324	MK, CW, WB, TC, TW, YL
120328	MK. CW, WB, TC, TW, YL
120330	MK, CW, WB, TC, TW, YL
120411	MK, WB, TC, TW, YL
120415	MK, CW, WB, TC, TW, YL
120417	CW
120423	CW, TC
120427	CW
120429	MK, CW, WB, TW, YL
120505	MK,CW, WB, TC, TW, YL
120509	MK, CW, WB, TC, TW, YL
120511	MK, CW, WB, TW, YL
120517	MK, CW, WB, TC, TW, YL
120523	MK, CW, WB, TC, TW, YL
120527	CW
120529	TC
120531	MK, CW, WB, TC, TW, YL
120604	WB, TC, TW, YL
120612	MK, CW, WB, TC, TW, YL
120616	MK, WB, TC, TW, YL
120616 BLANK	MK, CW, WB, TC, TW, YL
120620	MK, WB, TW, YL

Sampling Dates	Sampling Sites with Sample Collection
120630	TC
120710	WB, TW
120712	CW, WB, TC, TW, YL
120716	CW, TC, TW, YL
120722	MK, WB, TW, YL
120724	TW, YL
120728	MK, WB, TC, YL
120803	MK, CW, WB, TC, TW
120809	MK, WB, TC, YL
120815	MK, CW, WB, TC, TW, YL
120821	MK, CW, WB, TW
120827	MK, CW, WB, TC, TW, YL
120902	MK
120908	MK, CW, WB, TC, TW, YL
120914	MK, CW, WB, TC, TW, YL
120918	CW
120920	MK, WB, TW, YL
120923	MK, CW, WB, TW
120926	TC
121002	MK, CW, WB, TC, TW, YL
121008	MK, WB, TC, YL
121011	MK, CW, TW
121014	MK, CW, WB, TC, TW, YL
121014 BLANK	MK, CW, WB, TC, TW, YL
121018	CW, TC, YL
121020	CW, WB, TC, TW
121024	MK, CW, WB, TC, TW, YL
121026	CW, YL
121026 BLANK	MK, CW, WB, TC, TW, YL
121101	MK, CW, WB, TC, TW, YL
121105	MK, CW, WB, TC, TW, YL
121107	MK, CW, WB, TC, TW, YL
121113	MK, CW
121115	MK, CW, WB, TC, TW, YL

Sampling Dates	Sampling Sites with Sample Collection
121119	TC
121119 BLANK	MK, CW, WB, TC, TW, YL
121125	MK, CW, WB, TC, TW, YL
121129	MK, CW, WB, TC, TW, YL
121201	MK, CW, WB, TC, TW, YL
121204	MK, CW, WB, TC, TW, YL
121207	MK, CW, WB, TW, YL
121211	MK, CW, WB, TC, TW, YL
121213	MK, CW, WB, TC, TW, YL
121216	MK, WB, TC, TW, YL
121219	MK, CW, WB, TC, TW, YL
121225	MK, CW, WB, TC, TW, YL
121225 BLANK	MK, CW, WB, TC, TW, YL
121229	MK, CW, WB, TC, YL
121231	MK, CW, WB, TC, TW, YL

A total of 22 samples were identified to be invalid. The corresponding sample IDs, filter IDs, measured PM mass on both Teflon and QMA filters and the sum of measured chemical speices on the filter were listed in Table 5. A brief account for invalidating these samples is also provided in Table 5. The chemical data of these problematic filters will be included in the figure plotting (Figures 2 - 5 and 7) during the data validation in Section 3 but will be excluded from the linear regression analyses.

Table 5. List of invalid filter samples (Tender Ref. 11-03973).

Sample ID	Filter ID	PM Mass (Teflon), $\mu g/m^3$	PM Mass (QMA), $\mu g/m^3$	Sum of measured chemical species on the filter, $\mu g/m^3$	Remarks
MK120306ST01T	T0000050	0.588	57.542	0.028	visually observed to appear as non-sampled filter and proved by the chemical data
MK120821SQ01Q	Q0000411	20.000	22.625	23.068	abnormally high Ca^{2+} and NO_3^- concentrations and suspected to be contaminated
CW120324ST02T	T0000108	1.577	87.417	0.002	visually observed to appear as non-sampled filter and proved by the chemical data
CW120330SQ02Q	Q0000132	35.145	34.625	3.032	visually observed to appear as non-sampled filter and proved by the chemical data
CW120417SQ02Q	Q0000164	25.602	52.250	6.090	random areas of lighter deposit on the filter
CW120429SQ02Q	Q0000188	11.120	30.875	0.887	visually observed to appear as non-sampled filter and proved by the chemical data
CW120612SQ02Q	Q0000284	25.934	39.917	2.826	visually observed to appear as non-sampled filter and proved by the chemical data
CW120821SQ02Q	Q0000412	12.116	13.958	15.365	abnormally high Ca^{2+} and NO_3^- concentrations and suspected to be contaminated
CW120914ST02T	T0000439	115.270	44.833	5.478	chemical data showed that the weighing result of Teflon filter (115.27 $\mu g/m^3$) was too high and there is large discrepancy between the two collocated Teflon filter weighings (115.27 vs. 24.10 $\mu g/m^3$)
WB120821SQ03Q	Q0000413	12.792	14.000	15.413	abnormally high Ca^{2+} and NO_3^- concentrations and suspected to be contaminated
WB120821SC03Q	Q0000414	12.792	14.250	14.934	abnormally high Ca^{2+} and NO_3^- concentrations and suspected to be contaminated

Sample ID	Filter ID	PM Mass (Teflon), $\mu g/m^3$	PM Mass (QMA), $\mu g/m^3$	Sum of measured chemical species on the filter, $\mu g/m^3$	Remarks
WB120827SC03Q	Q0000422	34.417	39.417	31.278	abnormally high Ca^{2+} and NO_3^- concentrations and suspected to be contaminated
TC120827SQ04Q	Q0000423	35.667	38.750	33.608	abnormally high Ca^{2+} and NO_3^- concentrations and suspected to be contaminated
TC120827SC04Q	Q0000424	35.667	38.833	31.577	abnormally high Ca^{2+} and NO_3^- concentrations and suspected to be contaminated
TW120328SQ05Q	Q0000129	32.917	64.000	3.451	visually observed to appear as non-sampled filter and proved by the chemical data
TW120330SQ05Q	Q0000137	31.333	78.542	45.540	outliers in SO_4^{2-} vs. total S and K^+ vs. K and suspected to be contaminated
TW120815SQ05Q	Q0000417	24.708	28.083	27.164	abnormally high Ca^{2+} and NO_3^- concentrations and suspected to be contaminated
TW120821SQ05Q	Q0000425	15.583	19.417	18.025	abnormally high Ca^{2+} and NO_3^- concentrations and suspected to be contaminated
TW120827SQ05Q	Q0000425	38.958	43.667	37.467	abnormally high Ca^{2+} and NO_3^- concentrations and suspected to be contaminated
YL120531SQ06Q	Q0000266	25.375	18.625	1.248	visually observed to appear as non-sampled filter and proved by the chemical data
YL120815SQ06Q	Q0000410	27.625	27.167	28.893	abnormally high Ca^{2+} and NO_3^- concentrations and suspected to be contaminated
YL120827SQ06Q	Q0000426	41.958	44.958	38.133	abnormally high Ca^{2+} and NO_3^- concentrations and suspected to be contaminated

3. Database and Data Validation

3.1 Data File Preparation

An electronic database on analytical results is established for Hong Kong $PM_{2.5}$ data archive. Detailed data processing and data validation are documented in Section 3.3. The data are available on Compact Disc in the format of Microsoft Excel spreadsheets for convenient distribution to data users. The contents of the final data files are listed in Table 6.

Table 6. Summary of data files for the $PM_{2.5}$ study (EPD Tender Ref. 11-03973) in Hong Kong.

Category	Database File	File Description
I. DATABASE DOCUMENTATION		
	11-03973_ID.xls	Defines the field sample names, measurement units, and formats used in the database file
II. MASS AND CHEMICAL DATA		
	11-03973_PM2.5.xls	Contains $PM_{2.5}$ mass data and chemical data for samples collected by Partisol samplers at six sites once every six days during February 2012 to December 2012
III. DATABASE VALIDATION		
	11-03973_FLAG.xls	contains both field sampling and chemical analysis data validation flags

3.2 Measurement and Analytical Specifications

The measurement/analysis methods are described in Section 2 and every measurement consists of 1) a value; 2) a precision (uncertainty), and 3) a validity. The values are obtained by different analysis methods. The precisions are estimated through standard testing, blank analysis, and replicate analysis. The validity of each measurement is indicated by appropriate flagging in the data base, while the validity of chemical analysis results are evaluated by data validations described in Section 3.3.

A total of 61 sets of ambient $PM_{2.5}$ samples were received during this study and submitted for comprehensive chemical analyses. It is noted that each set of the ambient samples contains 16 pieces of filters collected at the six sampling sites but not necessarily on the same sampling date. These 61 sets of samples include 6 sets of field blanks. 4 out of 6 sites conducted collocated sampling and the collocated samples were used for data validation purpose. 954 out of the 976 $PM_{2.5}$ samples acquired are considered valid after data validation and final review.

3.2.1 Precision Calculations and Error Propagation

Measurement precisions are propagated from precisions of volumetric measurements, chemical composition measurements, and field blank variability using the methods of *Bevington* [1969] and *Watson et al.* [1995; 2001]. The following equations are used to calculate the prevision associated with filter-based measurements:

$$C_i = \frac{M_i - B_i}{V} \quad (1)$$

$$V = Q \times T \quad (2)$$

$$B_i = \frac{1}{n}\sum_{o=1}^{n} B_{io} \qquad for\ B_i > \sigma_{B_i} \quad (3)$$

$$B_i = 0 \qquad for\ B_i < \sigma_{B_i} \quad (4)$$

$$\sigma_{B_i} = STD_{B_i} = \left[\frac{i}{n-1}\sum_{o=1}^{n}\left(B_{io} - B_i\right)^2\right]^{\frac{1}{2}} \qquad for\ STD_{B_i} > SIG_{B_i} \quad (5)$$

$$\sigma_{B_i} = SIG_{B_i} = \left[\frac{i}{n}\sum_{o=1}^{n}\left(\sigma_{B_{io}}\right)^2\right]^{\frac{1}{2}} \qquad for\ STD_{B_i} \le SIG_{B_i} \quad (6)$$

$$\sigma_{C_i} = \left[\frac{\sigma_{M_i}^2 + \sigma_{B_i}^2}{V^2} + \frac{\sigma_V^2\left(M_i - B_i\right)^2}{V^4}\right]^{\frac{1}{2}} \quad (7)$$

$$\sigma_{RMSi} = \left(\frac{1}{n}\sum_{o=1}^{n}\sigma_{C_i}^2\right)^{\frac{1}{2}} \quad (8)$$

$$\frac{\sigma_V}{V} = 0.05 \quad (9)$$

where:

B_i = average amount of species *i* on field blanks

B_{io} = the amount of species *i* found on field blank *o*

C_i = the ambient concentration of species *i*

Q = flow rate throughout sampling period

M_i = amount of species *i* on the substrate

N = total number of samples in the sum

SIG_{Bi} = the root mean square error (RMSE), the square root of the averaged sum of the squared σ_{Bio}

STD_{Bio} = standard deviation of the blank

σ_{Bi} = blank precision for species *i*

σ_{Bio} = precision of the species *i* found on field blank *j*

σ_{Ci} = propagated precision for the concentration of species *i*

σ_{Mi} = precision of amount of species *i* on the substrate

σ_{RMSi} = root mean square precision for species *i*

σ_V = precision of sample volume

T = sample duration

V = volume of air sampled

The uncertainty of the measured value and the average uncertainty of the field blanks for each species are used to propagate the overall precision for each blank subtracted concentration value. The final value is propagated by taking the square root of the sum of the squares of the calculated uncertainty and the average field blank uncertainty for each measurement.

3.2.2 Analytical Specifications

The concentrations of field blanks collected during the study are summarized in Table 7 in the unit of μg/filter.

Blank precisions (σ_{Bi}) are defined as the higher value of the standard deviation of the blank measurements, STD_{Bi}, or the square root of the averaged squared uncertainties of the blank concentrations, SIG_{Bi}. If the average blank for a species was less than its precision, the blank was set to zero (Eqn 4).

The precisions (σ_{Mi}) were determined from duplicate analysis of samples. When duplicate sample analysis is made, the range of results, *R*, is nearly as efficient as the standard deviation since two measures differ by a constant (1.128*s* = *R* where *s* represents the precision).

Table 7. Field blank concentrations of $PM_{2.5}$ samples collected at MK, CW, WB, TC, TW, and YL sites during the study period in Hong Kong.

	Amounts in μg/47-mm filter					
Species	Total No. of Blanks	Field Blank Std. Dev. (STD_{Bi})	Root Mean Squared Blank Precision (SIG_{Bi})	Blank Precision (σ_{Bi})	Average Field Blank	Blank Subtracted (B_i)
Na^+	48	0.481	1.502	1.502	-0.345	0.000
NH_4^+	48	0.617	1.188	1.188	-1.422	0.000
K^+	48	0.263	1.726	1.726	-0.029	0.000
Cl^-	48	0.477	0.722	0.722	-0.005	0.000
NO_3^-	48	1.064	2.144	2.144	0.997	0.000
SO_4^{2-}	48	0.228	1.507	1.507	-0.154	0.000
OC1_TOR	48	0.279	2.428	2.428	0.630	0.000
OC2_TOR	48	1.607	2.599	2.599	4.033	4.033
OC3_TOR	48	1.483	2.603	2.603	4.110	4.110

Species	Amounts in µg/47-mm filter					
	Total No. of Blanks	Field Blank Std. Dev. (STD_{Bi})	Root Mean Squared Blank Precision (SIG_{Bi})	Blank Precision (σ_{Bi})	Average Field Blank	Blank Subtracted (B_i)
OC4_TOR	48	0.630	2.453	2.453	1.139	0.000
OC_TOR	48	4.255	3.008	4.255	12.088	12.088
OC_TOT	48	6.318	3.090	6.318	13.567	13.567
PyC_TOR	48	1.019	2.505	2.505	2.176	0.000
PyC_TOT	48	0.493	0.227	0.493	0.515	0.515
EC1_TOR	48	0.585	2.438	2.438	0.838	0.000
EC2_TOR	48	0.360	2.440	2.440	0.887	0.000
EC3_TOR	48	0.250	2.419	2.419	0.451	0.000
EC_TOR	48	0.002	2.396	2.396	0.000	0.000
EC_TOT	48	0.002	2.396	2.396	-0.001	0.000
TC	48	4.255	4.204	4.255	12.088	12.088
Na	48	0.1028	0.4111	0.4111	0.0750	0.0000
Mg	48	0.2094	1.7922	1.7922	0.4914	0.0000
Al	48	1.1114	0.5987	0.5987	0.1452	0.0000
Si	48	0.1250	0.6198	0.6198	-0.0240	0.0000
P	48	0.0202	0.0488	0.0488	-0.0148	0.0000
S	48	0.0059	0.0827	0.0827	0.0018	0.0000
Cl	48	0.0466	0.0934	0.0934	0.0282	0.0000
K	48	0.0428	0.0436	0.0436	0.0280	0.0000
Ca	48	0.0518	0.1272	0.1272	-0.0026	0.0000
Sc	48	0.0622	0.5007	0.5007	0.2174	0.0000
Ti	48	0.0125	0.0360	0.0360	0.0103	0.0000
V	48	0.0060	0.0135	0.0135	-0.0059	0.0000
Cr	48	0.0092	0.0212	0.0212	0.0099	0.0000
Mn	48	0.0305	0.1195	0.1195	0.0516	0.0000
Fe	48	0.0547	0.1356	0.1356	-0.0253	0.0000
Co	48	0.0088	0.0261	0.0261	0.0028	0.0000
Ni	48	0.0083	0.0267	0.0267	0.0094	0.0000
Cu	48	0.0287	0.0475	0.0475	0.0227	0.0000
Zn	48	0.0291	0.2055	0.2055	0.0078	0.0000

Species	Amounts in µg/47-mm filter					
	Total No. of Blanks	Field Blank Std. Dev. (STD_{Bi})	Root Mean Squared Blank Precision (SIG_{Bi})	Blank Precision (σ_{Bi})	Average Field Blank	Blank Subtracted (B_i)
Ga	48	0.0238	0.0743	0.0743	0.0212	0.0000
Ge	48	0.0225	0.0855	0.0855	-0.0115	0.0000
As	48	0.0005	0.0066	0.0066	0.0001	0.0000
Se	48	0.0000	0.0343	0.0343	0.0000	0.0000
Br	48	0.0126	0.0275	0.0275	-0.0122	0.0000
Rb	48	0.0157	0.0515	0.0515	0.0023	0.0000
Sr	48	0.0197	0.0230	0.0230	-0.0097	0.0000
Y	48	0.0045	0.0991	0.0991	-0.0051	0.0000
Zr	48	0.0447	0.0862	0.0862	0.0226	0.0000
Nb	48	0.0342	0.0753	0.0753	-0.0410	0.0000
Mo	48	0.0279	0.0946	0.0946	-0.0626	0.0000
Rh	48	0.0608	0.1884	0.1884	0.0665	0.0000
Pd	48	0.0558	0.0578	0.0578	-0.1250	0.0000
Ag	48	0.0418	0.1105	0.1105	0.0234	0.0000
Cd	48	0.0487	0.1715	0.1715	0.0390	0.0000
In	48	0.0606	0.2503	0.2503	0.0046	0.0000
Sn	48	0.0782	0.2435	0.2435	-0.0575	0.0000
Sb	48	0.0666	0.2775	0.2775	0.0301	0.0000
Te	48	0.0848	0.2451	0.2451	-0.0561	0.0000
I	48	0.1226	1.5314	1.5314	0.0948	0.0000
Cs	48	0.2077	2.4325	2.4325	0.8440	0.0000
Ba	48	0.2851	2.8833	2.8833	1.2549	0.0000
La	48	0.3336	0.9433	0.9433	1.2750	1.2750
Ce	48	0.0222	0.0730	0.0730	0.0200	0.0000
Sm	48	0.0394	0.2197	0.2197	0.0290	0.0000
Eu	48	0.0672	0.0618	0.0672	-0.0391	0.0000
Tb	48	0.0271	0.5384	0.5384	-0.0015	0.0000
Hf	48	0.1365	0.3341	0.3341	0.1834	0.0000
Ta	48	0.0461	0.5979	0.5979	0.0167	0.0000
W	48	0.1817	0.2036	0.2036	0.3958	0.3958
Ir	48	0.0344	0.0190	0.0344	-0.0515	0.0000

Species	Amounts in µg/47-mm filter					
	Total No. of Blanks	Field Blank Std. Dev. (STD_{Bi})	Root Mean Squared Blank Precision (SIG_{Bi})	Blank Precision (σ_{Bi})	Average Field Blank	Blank Subtracted (B_i)
Au	48	0.0370	0.0074	0.0370	0.0181	0.0000
Hg	48	0.0073	0.0863	0.0863	0.0010	0.0000
Tl	48	0.0289	0.1005	0.1005	0.0183	0.0000
Pb	48	0.0394	0.1095	0.1095	-0.0189	0.0000
U	48	0.0496	0.0161	0.0496	-0.0641	0.0000

The analytical specifications for the 24-hour $PM_{2.5}$ measurements obtained during the study are summarized in Table 8. Limits of detection (LOD) and limits of quantitation (LOQ) are given. The LOD of an analyte may be described as that concentration which gives an instrument signal significantly different from the "blank" or "background" signal. In this study LOD is defined as the concentration at which instrument response equals three times the standard deviation of the concentrations of low level standards. As a further limit, the LOQ is regarded as the lower limit for precise quantitative measurements and is defined as a concentration corresponding to ten times the standard deviation of the concentrations of low level standards. The LOQs should always be equal to or larger than the analytical LODs and it was the case for all the chemical compounds listed in Table 6. Both the LODs and LOQs in µg/m^3 were obtained by divided the LODs and LOQs in µg/filter by 24.0 m^3, the nominal 24-hour volume, for the Partisol samplers. The variation of sampling volumes is assumed to be within ±5% of the pre-set volume.

Table 8. Analytical specifications of 24-hour $PM_{2.5}$ measurements at MK, CW, WB, TC, TW, and YL sites during the study period in Hong Kong.

Species	Analytical Method	LOD (µg/m^3)	LOQ (µg/m^3)	No. of valid Values	No. > LOD	% > LOD	No. > LOQ	% > LOQ
Na^+	IC	0.016	0.052	311	285	92%	285	92%
NH_4^+	IC	0.012	0.041	311	311	100%	311	100%
K^+	IC	0.018	0.060	311	291	94%	291	94%
Cl^-	IC	0.008	0.025	311	205	66%	205	67%
NO_3^-	IC	0.022	0.074	311	308	99%	308	99%
SO_4^{2-}	IC	0.016	0.052	311	311	100%	311	100%
OC1_TOR	TOR	0.034	0.112	311	22	7%	1	0%
OC2_TOR	TOR	0.061	0.204	311	310	100%	302	97%
OC3_TOR	TOR	0.079	0.263	311	311	100%	311	100%
OC4_TOR	TOR	0.166	0.553	311	303	97%	159	51%

Species	Analytical Method	LOD (µg/m^3)	LOQ (µg/m^3)	No. of valid Values	No. > LOD	% > LOD	No. > LOQ	% > LOQ
OC_TOR	TOR	0.327	1.090	311	311	100%	311	95%
OC_TOT	TOT	0.135	0.450	311	311	100%	311	100%
PyC_TOR	TOR	0.089	0.297	311	303	97%	281	90%
PyC_TOT	TOT	0.029	0.096	311	300	96%	290	93%
EC1_TOR	TOR	0.047	0.158	311	310	100%	307	99%
EC2_TOR	TOR	0.034	0.112	311	311	100%	311	100%
EC3_TOR	TOR	0.028	0.092	311	310	100%	273	88%
EC_TOR	TOR	0.002	0.006	311	311	100%	311	100%
EC_TOT	TOT	0.001	0.002	311	311	100%	311	100%
TC	TOR	0.327	1.088	311	311	100%	311	100%
Na	XRF	0.0126	0.0418	311	310	100	310	100
Mg	XRF	0.0566	0.1886	311	310	100	164	53
Al	XRF	0.0227	0.0756	311	310	100	256	82
Si	XRF	0.0261	0.0869	311	302	97	257	83
P	XRF	0.0022	0.0074	311	299	96	244	78
S	XRF	0.0034	0.0114	311	311	100	311	100
Cl	XRF	0.0037	0.0122	311	305	98	237	76
K	XRF	0.0016	0.0053	311	311	100	311	100
Ca	XRF	0.0053	0.0177	311	311	100	308	99
Sc	XRF	0.0185	0.0617	311	0	0	0	0
Ti	XRF	0.0014	0.0048	311	298	96	226	73
V	XRF	0.0006	0.0020	311	310	100	306	98
Cr	XRF	0.0008	0.0028	311	232	75	95	31
Mn	XRF	0.0045	0.0151	311	269	86	153	49
Fe	XRF	0.0058	0.0194	311	310	100	304	98
Co	XRF	0.0011	0.0036	311	19	6	0	0
Ni	XRF	0.0011	0.0035	311	305	98	197	63
Cu	XRF	0.0018	0.0061	311	305	98	249	80
Zn	XRF	0.0085	0.0283	311	301	97	269	86
Ga	XRF	0.0028	0.0094	311	11	4	0	0
Ge	XRF	0.0036	0.0122	311	4	1	0	0
As	XRF	0.0003	0.0009	311	160	51	151	49
Se	XRF	0.0000	0.0000	311	4	1	4	1

Species	Analytical Method	LOD (µg/m^3)	LOQ (µg/m^3)	No. of valid Values	No. > LOD	% > LOD	No. > LOQ	% > LOQ
Br	XRF	0.0014	0.0048	311	279	90	228	73
Rb	XRF	0.0013	0.0043	311	98	32	5	2
Sr	XRF	0.0021	0.0070	311	140	45	5	2
Y	XRF	0.0010	0.0034	311	17	5	0	0
Zr	XRF	0.0042	0.0139	311	43	14	0	0
Nb	XRF	0.0033	0.0111	311	1	0	0	0
Mo	XRF	0.0035	0.0118	311	8	3	0	0
Rh	XRF	0.0046	0.0152	311	41	13	0	0
Pd	XRF	0.0071	0.0235	311	0	0	0	0
Ag	XRF	0.0037	0.0125	311	17	5	0	0
Cd	XRF	0.0043	0.0144	311	41	13	0	0
In	XRF	0.0066	0.0220	311	2	1	0	0
Sn	XRF	0.0104	0.0346	311	79	25	1	0
Sb	XRF	0.0108	0.0361	311	12	4	0	0
Te	XRF	0.0112	0.0373	311	1	0	0	0
I	XRF	0.0109	0.0364	311	50	16	0	0
Cs	XRF	0.0617	0.2057	311	7	2	0	0
Ba	XRF	0.0776	0.2586	311	61	20	0	0
La	XRF	0.0870	0.2901	311	0	0	0	0
Ce	XRF	0.0019	0.0064	311	22	7	0	0
Sm	XRF	0.0028	0.0095	311	82	26	0	0
Eu	XRF	0.0088	0.0295	311	16	5	0	0
Tb	XRF	0.0029	0.0097	311	76	24	11	4
Hf	XRF	0.0224	0.0748	311	2	1	0	0
Ta	XRF	0.0120	0.0399	311	35	11	0	0
W	XRF	0.0247	0.0825	311	0	0	0	0
Ir	XRF	0.0042	0.0141	311	0	0	0	0
Au	XRF	0.0012	0.0040	311	13	4	4	1
Hg	XRF	0.0000	0.0000	311	1	0	1	0
Tl	XRF	0.0036	0.0120	311	0	0	0	0
Pb	XRF	0.0040	0.0135	311	253	81	203	65
U	XRF	0.0047	0.0157	311	2	1	0	0

The number of reported concentrations for each species and number of reported concentrations greater than the LODs and LOQs are also summarized in Table 8. For the 311 valid samples, major ions (including nitrate, sulfate, ammonium, soluble sodium, and soluble potassium), organic carbon, elemental carbon, sodium (Na), magnesium (Mg), aluminum (Al), silicon (Si), phosphorus (P), sulfur (S), chlorine (Cl), potassium (K), calcium (Ca), titanium (Ti), vanadium (V), iron (Fe), nickel (Ni), copper (Cu) and zinc (Zn) were detected (> LOD) in almost all samples (more than 90%). Chloride was detected in 67% of the samples. Several transition metals (e.g. Sc, Co, Y, Nb, Mo, Pd, Ag, Cd, Hf, Ta, W, Ir, Au, Hg, La, Ce and U) were not detected in most of the samples (less than 15%). Species from motor vehicle exhaust such as Br and Pb were detected in 90% and 81% of the samples respectively. V and Ni, which are residual-oil-related species, were detected in 100% and 98% of the samples, respectively. This is typical for urban and suburban sites in most regions. Toxic species emitted from industrial sources, such as Cd and Hg, were not detected (13% and 0% of the samples, respectively). Soil-dust-related species, including Al, Si, Ca, Ti, and Fe, were found above the LODs in more than 96% of the samples and above the LOQs in more than 73% of the samples.

In general, the analytical specifications shown in Table 8 suggest that the $PM_{2.5}$ samples collected during the study period possess adequate loading for chemical analysis. The detection limits of the selected analytical methods were sufficiently low to establish valid measurements with acceptable precision.

3.3 Data Validation

Three levels of data validation were conducted to the data acquired from the study.

Level I data validation: 1) flag measurements for deviations from procedures; 2) identify and remove invalid values and indicate the reasons for invalid sampling, and 3) estimate precisions from replicate and blank analyses.

Level II data validation examines internal consistency tests among different data and attempts to resolve discrepancies based on known physical relationships between variables: 1) compare a sum of chemical species to mass concentrations; 2) compare measurements from different methods; 3) compare collocated measurements; 4) examine time series from different sites to identify and investigate outliers, and 5) prepare a data qualification statement.

Level III data validation is part of the data interpretation process and should identify unusual values including: 1) extreme values; 2) values which would otherwise normally track the values of other variables in a time series, and 3) values for observables which would normally follow a qualitatively predictable spatial or temporal pattern. External consistency tests are used to identify values in the data set which appear atypical when compared to other data sets. The first assumption upon finding a measurement which is inconsistent with physical expectations is that the unusual value is due to a measurement error. If nothing unusual is found upon tracing the path of the measurement, the value would be assumed to be a valid result of an environmental cause.

Level I data validation was performed and the validation flags and comments are stated in the database as documented in Section 3.1. Level II validation tests and results are described in the following subsections including 1) sum of chemical species versus $PM_{2.5}$

mass; 2) physical and chemical consistency; 3) anion/cation balance; 4) reconstructed versus measured mass, 5) carbon measurements by different thermal/optical methods, and 6) collocated measurement comparison. For Level III data validation, parallel consistency tests were applied to data sets from the same population (e.g., region, period of time) by different data analysis approaches. Collocated samples collected at four out of the six sampling sites were examined. Comparison of $PM_{2.5}$ mass concentrations obtained from gravimetric analysis and from 24-hr average TEOM measurements were also conducted. The level III data validation continues for as long as the database is maintained. For Level II/III data validation in this study, correlations and linear regression statistics were performed on the valid data set and scatter plots were generated for better comparison.

3.3.1 Sum of Chemical Species versus $PM_{2.5}$ Mass

The sum of the individual chemical concentrations determined in this study for $PM_{2.5}$ samples should be less than or equal to the corresponding mass concentrations obtained from gravimetric measurements. The chemical species include those that were quantified on both Teflon-membrane filters and quartz fiber filters. To avoid double counting, chloride (Cl^-), total potassium (K), soluble sodium (Na^+), and sulfate (SO_4^{2-}) are included in the sum while total sulfur (S), total chlorine (Cl), total sodium (Na), and soluble potassium (K^+) are excluded. Carbon concentration is represented by the sum of organic carbon and elemental carbon. Unmeasured ions, metal oxides, or hydrogen and oxygen associated with organic carbon are not counted into the measured concentrations.

The sum of chemical species was plotted against the measured $PM_{2.5}$ mass on Teflon filters for each of the individual sites in Figure 2. Linear regression analysis results and the average ratios of Y over X are both shown in Table 9 for comparison. Each plot contains a solid line indicating the slope with intercept and a dashed 1:1 line. Measurement uncertainties associated with the x- and y-axes are shown and the uncertainties of the PM mass data were assumed to be 5% of the concentrations.

A strong correlation (R^2 = 0.98) was found between the sum of measured species and mass with a slope of 0.80 ± 0.01. The average Y/X ratios indicate that approximately 79 - 89% of the $PM_{2.5}$ mass can be explained by the measured chemical species.

The sum of species measured on TW120330 is more than the corresponding $PM_{2.5}$ mass beyond the reported measurement uncertainties. The $PM_{2.5}$ mass concentration determined for TW120330 is 31.33 μg/m^3 on Teflon filter, 78.54 μg/m^3 on QMA filter, and 45.54 μg/m^3 for sum-of-species, respectively. Good agreements were observed for this sample in NH_4^+ balance, charge balance, and carbon concentration comparison while large deviations were found in SO_4^{2-} vs. total S and K^+ vs. total K. This indicates that chemical analysis of the QMA filter is reliable but the sampling loadings on Teflon filter and QMA filter are likely different. It is suspected that this sample was contaminated during sample delivery and/or storage. Hence TW120330 is considered as invalid sample.

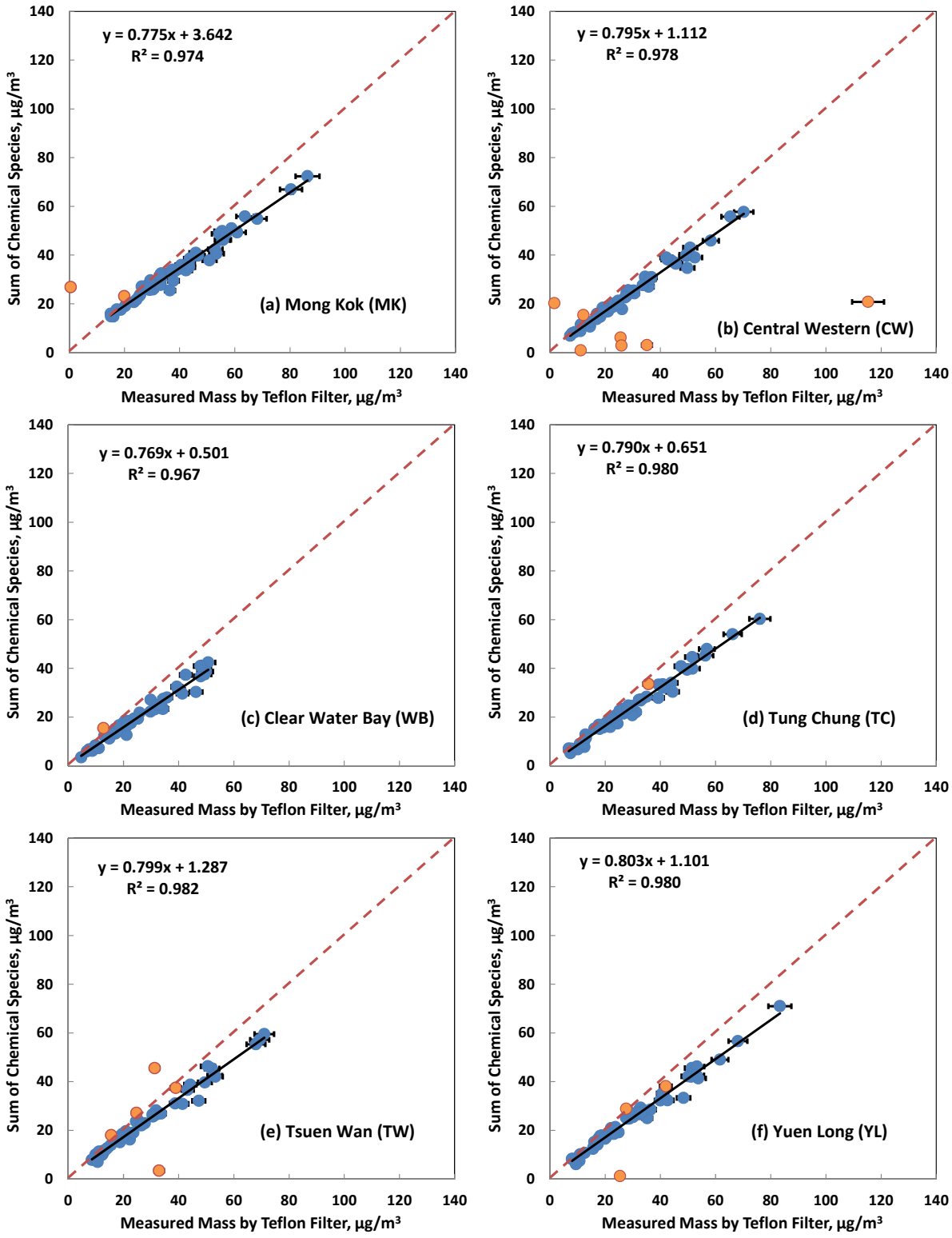

Figure 2. Scatter plots of sum of measured chemical species versus measured mass on Teflon filter for $PM_{2.5}$ samples collected at (a) MK, (b) CW, (c) WB, (d) TC, (e) TW, and (f) YL (Orange dots are measurements for samples that are identified to be invalid, the same hereinafter).

Table 9. Statistics analysis of sum of measured chemical species versus measured mass on Teflon filters for $PM_{2.5}$ samples collected at individual sites.

Statistics/Site	MK	CW	WB	TC	TW	YL	ALL
n	53	48	54	54	50	52	311
Slope	0.775 (± 0.018)	0.795 (± 0.018)	0.769 (± 0.020)	0.790 (± 0.016)	0.799 (± 0.016)	0.802 (± 0.016)	0.804 (± 0.007)
Intercept	3.642 (± 0.754)	1.112 (± 0.609)	0.501 (± 0.561)	0.651 (± 0.517)	1.287 (± 0.514)	1.129 (± 0.559)	0.889 (± 0.256)
R^2	0.974	0.978	0.967	0.980	0.982	0.980	0.974
AVG mass	38.934	30.866	25.482	29.070	28.644	30.153	30.518
AVG sum	33.830	25.648	20.086	23.619	24.171	25.317	25.432
AVG sum/mass	0.887 (± 0.074)	0.843 (± 0.068)	0.793 (± 0.073)	0.821 (± 0.083)	0.859 (± 0.072)	0.852 (± 0.079)	0.842 (± 0.080)

3.3.2 Physical and Chemical Consistency

Measurements of chemical species concentrations conducted by different methods are compared. Physical and chemical consistency tests include: 1) sulfate (SO_4^{2-}) versus total sulfur (S); 2) soluble potassium (K^+) versus total potassium (K), and 3) chloride (Cl^-) versus total chlorine (Cl).

3.3.2.1 Water-Soluble Sulfate (SO_4^{2-}) versus Total Sulfur (S)

SO_4^{2-} is measured by ion chromatography (IC) on QMA filters and total S is measured by x-ray fluorescence (XRF) on Teflon filters. The ratio of SO_4^{2-} to S is expected to equal three if all of the sulfur is present as SO_4^{2-}. Figure 3 shows the scatter plots of SO_4^{2-} versus total S concentrations for each of the six sites. A good correlation (R^2 = 0.97) were observed for all the sites with a slope of 3.17 ± 0.03 and an intercept of -0.72 ± 0.11. The average sulfate to total sulfur ratio was determined to be 2.90 ± 0.25, which meets the validation criteria (SO_4^{2-}/total S < 3.0).

Good correlations (R^2 = 0.96 - 0.98) were found for sulfate/total sulfur in $PM_{2.5}$ samples collected in individual sites. The regression statistics suggest a slope ranging from 2.96 ± 0.06 to 3.38 ± 0.08 and the intercepts are all at relatively low levels. The average sulfate/sulfur ratio ranges from 2.88 ± 0.26 to 2.92 ± 0.26. Both of the calculations indicate that most of the sulfur was present as soluble sulfate in $PM_{2.5}$.

The outliers found in Figure 3e are ascribed to TW120328 and TW120330. For the TW120330 sample, the ammonium balance and charge balance calculated from the ion concentrations were examined (Sections 3.3.2.4 & 3.3.2.5) and they suggest the validity of the IC analysis. Considering the much higher mass concentrations found on QMA filter (78.542 μg/m^3) than that on Teflon filter (31.333 μg/m^3), it is suspected that the sampling loadings on Teflon filter and QMA filter are different. The QMA filter sample might be contaminated during sample delivery and/or storage.

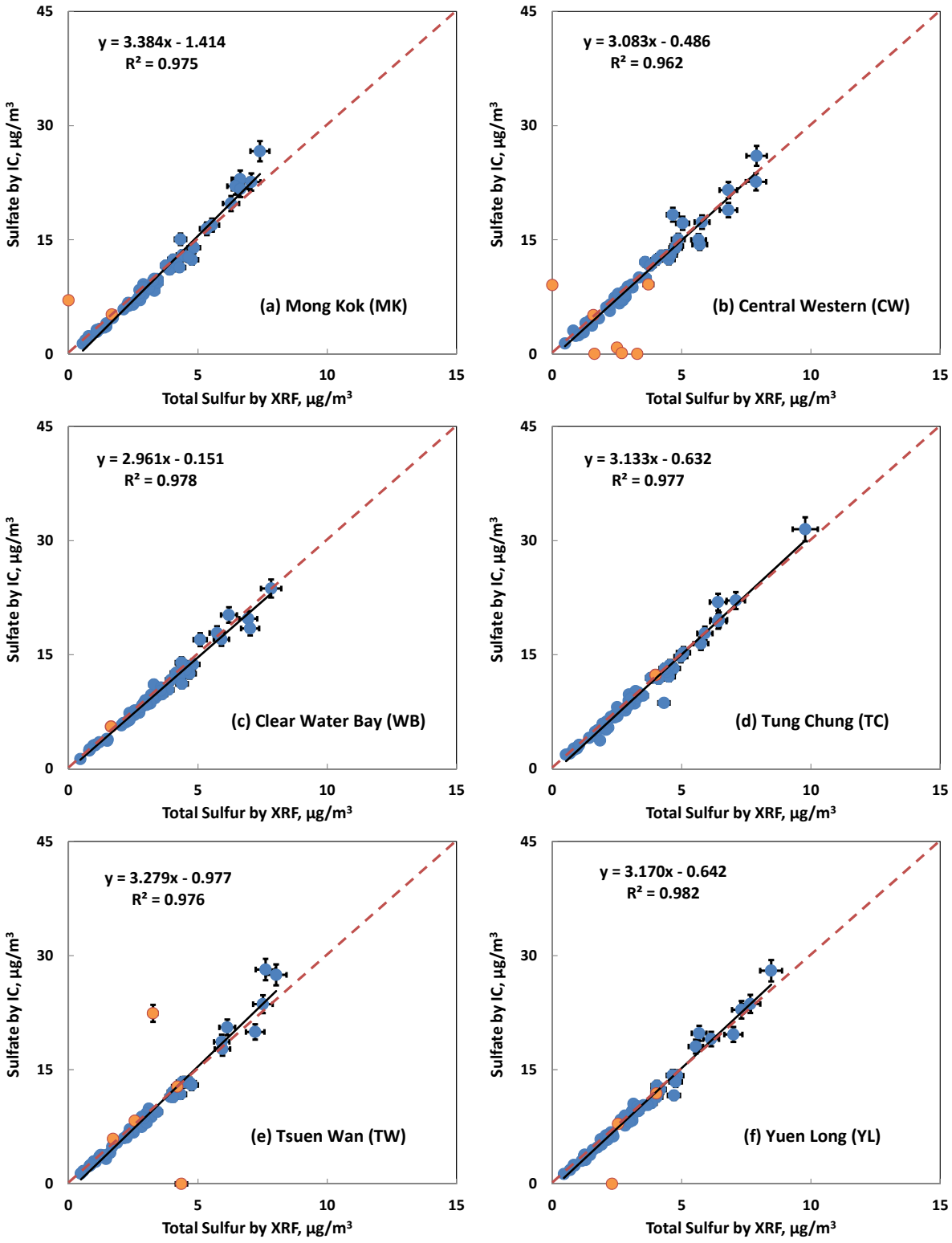

Figure 3. Scatter plots of sulfate versus total sulfur measurements for $PM_{2.5}$ samples collected at (a) MK, (b) CW, (c) WB, (d) TC, (e) TW, and (f) YL.

Table 10. Statistics analysis of sulfate versus total sulfur measurements for $PM_{2.5}$ samples collected at individual sites.

Statistics/Site	MK	CW	WB	TC	TW	YL	ALL
n	53	48	54	54	50	52	311
Slope	3.384 (± 0.076)	3.083 (± 0.090)	2.961 (± 0.061)	3.133 (± 0.067)	3.279 (± 0.075)	3.170 (± 0.061)	3.170 (± 0.030)
Intercept	-1.414 (± 0.289)	-0.486 (± 0.352)	-0.151 (± 0.222)	-0.632 (± 0.255)	-0.977 (± 0.277)	-0.642 (± 0.225)	-0.723 (± 0.112)
R^2	0.975	0.962	0.978	0.977	0.976	0.982	0.973
AVG total S	3.377	3.464	3.205	3.331	3.168	3.226	3.294
AVG SO_4^{2-}	10.015	10.194	9.338	9.804	9.411	9.583	9.719
AVG SO_4^{2-}/S	2.875 (± 0.261)	2.902 (± 0.316)	2.906 (± 0.197)	2.922 (± 0.262)	2.901 (± 0.229)	2.916 (± 0.222)	2.904 (± 0.248)

3.3.2.2 Water-soluble Potassium (K^+) versus Total Potassium (K)

Water-soluble potassium (K^+) is measured by ion chromatography (IC) on QMA filters and the total potassium (K) is measured by x-ray fluorescence (XRF) on Teflon filters. The ratio of K^+ to K is expected to equal or be less than 1. Figure 4 shows the scatter plots of K^+ versus total K concentrations for each of the six sites. A fairly good correlation (R^2 = 0.84) were observed for all the sites with a slope of 0.92 ± 0.02 and an intercept of 0.02 ± 0.01. The ratio of water-soluble potassium to total potassium averages at 1.08 ± 0.59.

Good correlations (R^2 = 0.77 - 0.90) were found for K^+/K in $PM_{2.5}$ samples collected in individual sites. The regression statistics suggest a slope ranging from 0.77 ± 0.05 to 0.96 ± 0.07 and the intercepts are all at relatively low levels. The circled dots represent the samples collected at MK, WB, TC, TW and YL sites on March 24, 2012. Hong Kong was under the influence of dust storm coming from the Northern China. The concentrations of soluble potassium ion were only approx. 50% of those of total potassium, leading to the great deviation of K^+/K ratio from the 1:1 line.

Generally, almost all of the total potassium is in its soluble ionic form and a few scattered data points might be caused by instrumental and method uncertainties.

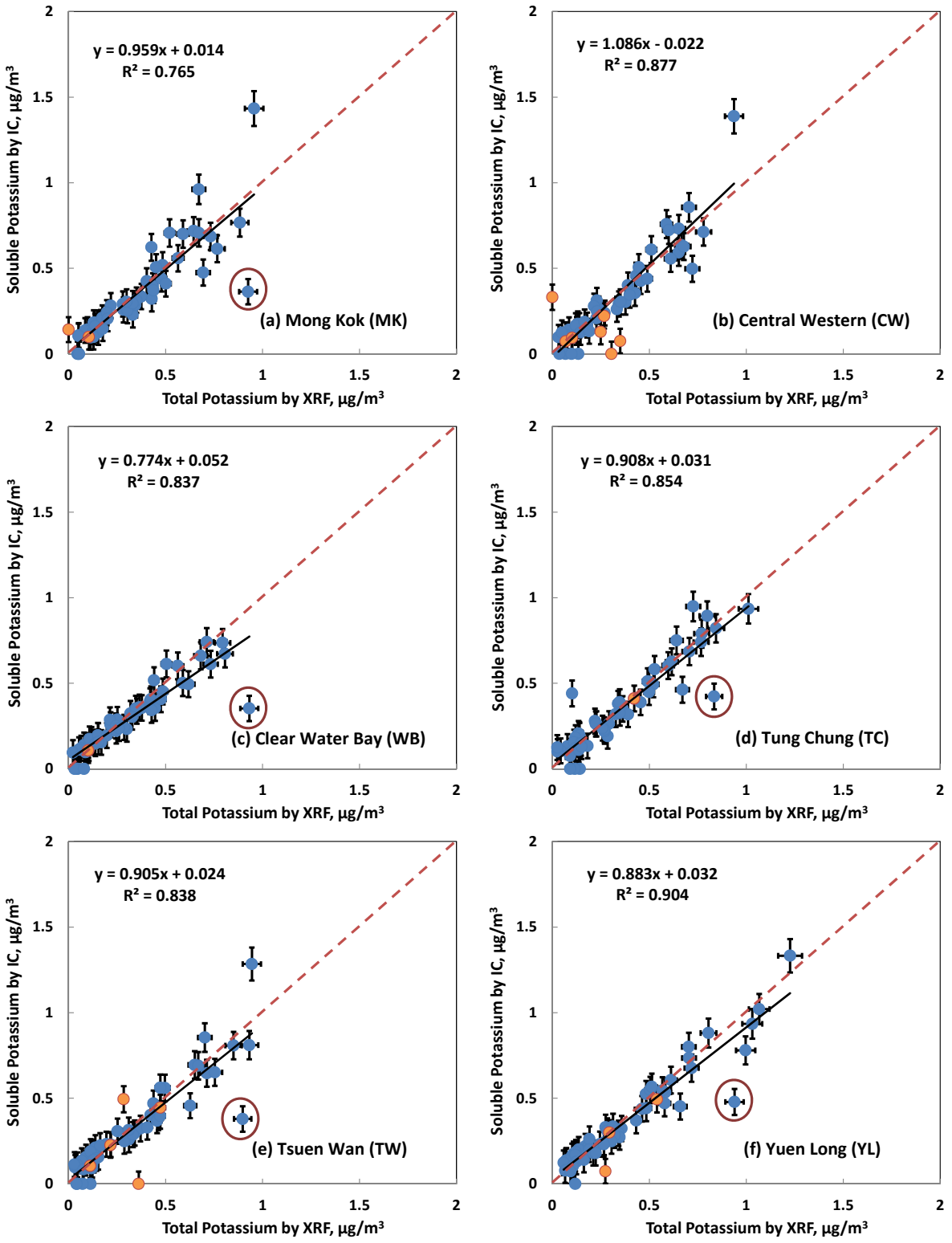

Figure 4. Scatter plots of water-soluble potassium versus total potassium measurements for $PM_{2.5}$ samples collected at (a) MK, (b) CW, (c) WB, (d) TC, (e) TW, and (f) YL. The circled samples were collected on a day (March 24, 2012) influenced by dust storm.

Table 11. Statistics analysis of water-soluble potassium versus total potassium measurements for $PM_{2.5}$ samples collected at individual sites.

Statistics/Site	MK	CW	WB	TC	TW	YL	ALL
n	53	48	54	54	50	52	311
Slope	0.959 (± 0.074)	1.086 (± 0.060)	0.774 (± 0.047)	0.908 (± 0.052)	0.905 (± 0.057)	0.883 (± 0.041)	0.915 (± 0.023)
Intercept	0.014 (± 0.032)	-0.022 (± 0.025)	0.052 (± 0.018)	0.031 (± 0.022)	0.024 (± 0.024)	0.032 (± 0.020)	0.024 (± 0.010)
R^2	0.765	0.877	0.837	0.854	0.838	0.904	0.840
AVG total K	0.349	0.337	0.304	0.344	0.325	0.387	0.341
AVG K^+	0.349	0.344	0.288	0.344	0.318	0.374	0.336
AVG K^+/K	1.017 (± 0.398)	1.047 (± 0.522)	1.042 (± 0.618)	1.187 (± 0.867)	1.101 (± 0.645)	1.060 (± 0.349)	1.076 (± 0.592)

3.3.2.3 Water-soluble Chloride (Cl^-) versus Total Chlorine (Cl)

Water-soluble chloride (Cl^-) is measured by ion chromatography (IC) on QMA filters and the total chlorine (Cl) is measured by x-ray fluorescence (XRF) on Teflon filters. The ratio of Cl^- to Cl is expected to equal or be less than 1. Figure 5 shows the scatter plots of Cl^- versus total Cl concentrations for each of the six sites. Moderate correlations (R^2 = 0.45) were found for the combined data of all the sampling sites. The slopes were larger than unity (1.25 - 2.70) except for the TW site (0.84), of which the slope was significantly affected by the data point with very high Cl and Cl^- concentrations. The uncertainties of Cl measurements are mainly associated itsvolatility. On one hand, a portion of Cl^- could be lost during the storage of the QMA filters especially when the aerosol samples are acidic. On the other hand, some Cl would be volatized in the vacuum chamber during XRF analysis. Such losses are more significant when chlorine concentrations are low. The degree of both losses is unknown and the data appear to suggest that the loss during XRF analysis is more significant.

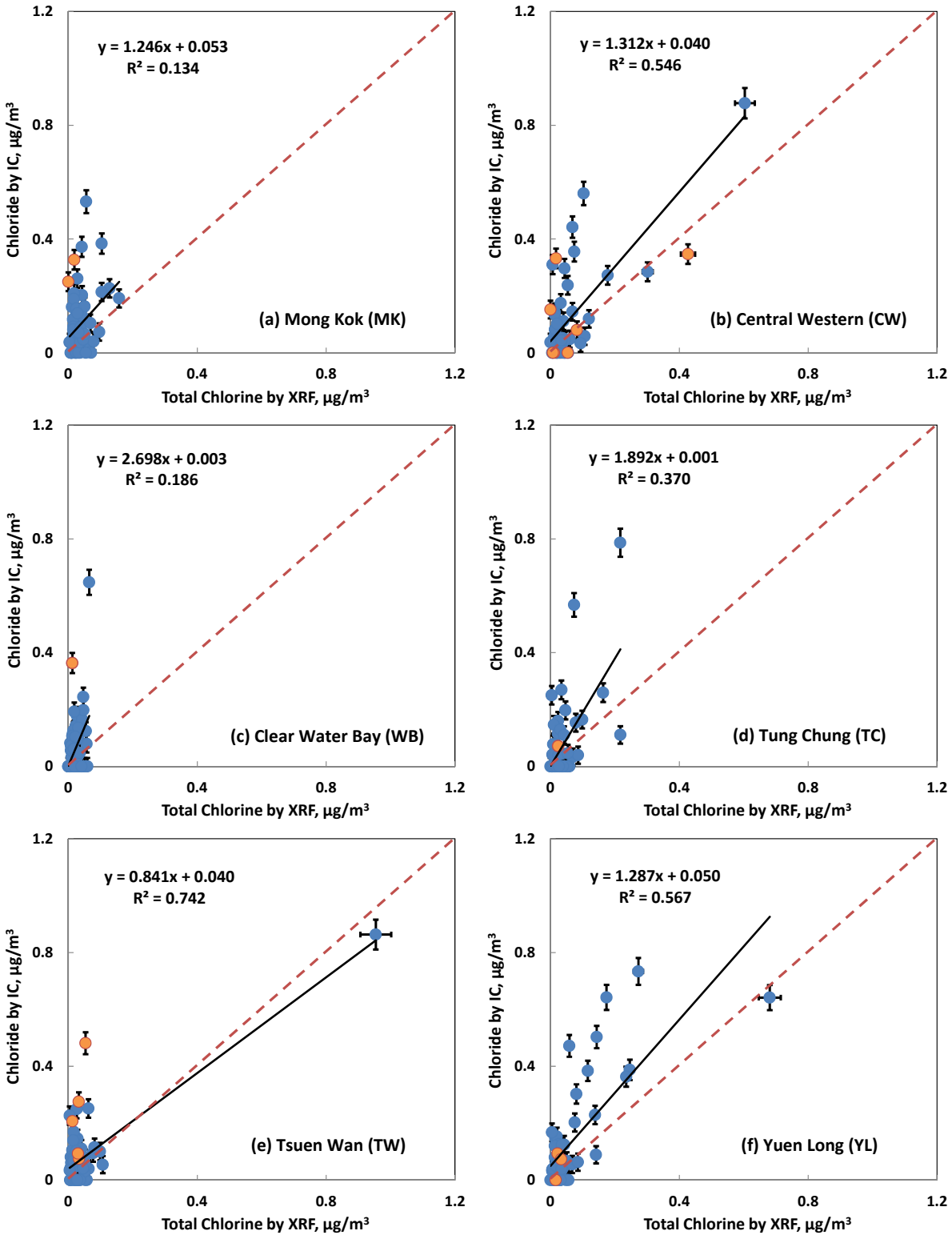

Figure 5. Scatter plots of water-soluble chloride versus total chlorine measurements for $PM_{2.5}$ samples collected at (a) MK, (b) CW, (c) WB, (d) TC, (e) TW, and (f) YL.

Table 12. Statistics analysis of water-soluble chloride versus total chlorine measurements for $PM_{2.5}$ samples collected at individual sites.

Statistics/Site	MK	CW	WB	TC	TW	YL	ALL
n	53	48	54	54	50	52	311
Slope	1.246 (± 0.443)	1.312 (± 0.176)	2.698 (± 0.782)	1.892 (± 0.342)	0.841 (± 0.072)	1.287 (± 0.159)	1.157 (± 0.073)
Intercept	0.053 (± 0.022)	0.040 (± 0.019)	0.003 (± 0.022)	0.001 (± 0.020)	0.040 (± 0.010)	0.050 (± 0.020)	0.043 (± 0.007)
R^2	0.134	0.546	0.186	0.370	0.742	0.567	0.447
AVG total Cl	0.039	0.057	0.024	0.038	0.050	0.063	0.045
AVG Cl^-	0.102	0.116	0.067	0.072	0.082	0.131	0.094
AVG Cl^-/Cl	3.421 (± 3.553)	3.398 (± 6.749)	3.097 (± 3.477)	2.861 (± 8.871)	3.971 (± 7.876)	3.167 (± 5.182)	3.314 (± 6.248)

3.3.2.4 Ammonium Balance

To further validate the ion measurements, calculated versus measured ammonium (NH_4^+) are compared. NH_4^+ is directly measured by IC analysis of QMA filter extract. NH_4^+ is very often found in the chemical forms of NH_4NO_3, $(NH_4)_2SO_4$, and NH_4HSO_4 while NH_4Cl is usually negligible and excluded from the calculation. Assuming full neutralization, measured NH_4^+ can be compared with the computed NH_4^+, which can be calculated in the following two ways,

Calculated NH_4^+ based on NH_4NO_3 and $(NH_4)_2SO_4 = 0.29 \times NO_3^- + 0.38 \times SO_4^{2-}$

Calculated NH_4^+ based on NH_4NO_3 and $NH_4HSO_4 = 0.29 \times NO_3^- + 0.192 \times SO_4^{2-}$

The calculated NH_4^+ is plotted against measured NH_4^+ for each of the six sites in Figure 6. For both forms of sulfate the comparisons show strong correlations (R^2 = 0.98 for ammonium sulfate and R^2 = 0.96 for ammonium bisulfate, respectively) but with quite different slopes. The slopes for individual sampling sites range from 1.01 ± 0.02 at MK to 1.11 ± 0.03 at WB assuming ammonium sulfate, and from 0.53 ± 0.01 at MK to 0.59 ± 0.02 at YL assuming ammonium bisulfate. These values were close to those found in earlier years. The average ratios of calculated ammonium to measured ammonium suggest that ammonium sulfate is the dominant form for sulfate in the $PM_{2.5}$ over the Hong Kong region in the year of 2012.

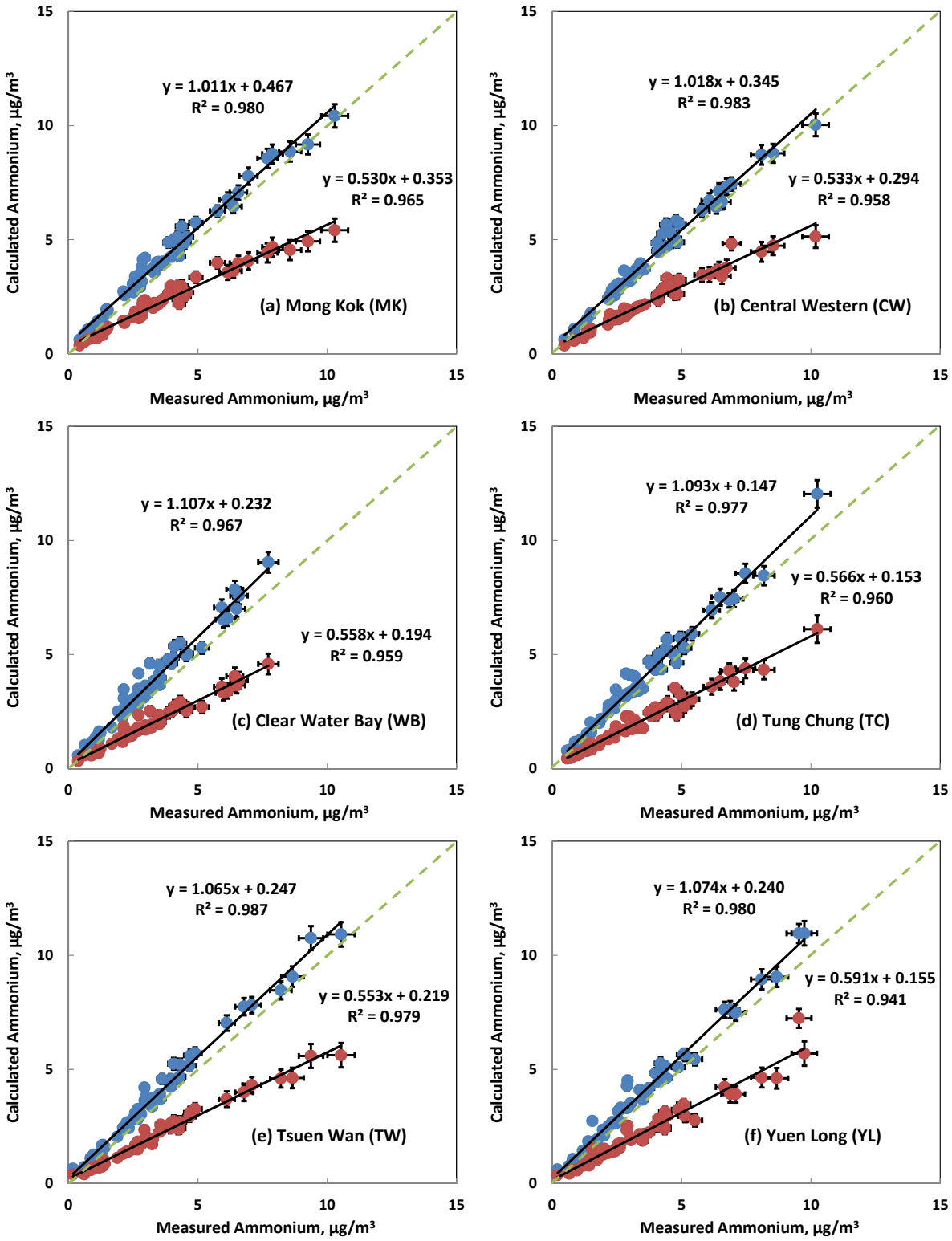

Figure 6. Scatter plots of calculated ammonium versus measured ammonium for PM2.5 samples collected at (a) MK, (b) CW, (c) WB, (d) TC, (e) TW, and (f) YL. The calculated ammonium data are obtained assuming all nitrate was in the form of ammonium nitrate and all sulfate was in the form of either ammonium sulfate (data in blue) or ammonium bisulfate (data in brown).

Table 13. Statistics analysis of calculated ammonium versus measured ammonium for $PM_{2.5}$ samples collected at individual sites.

Statistics/Site	MK	CW	WB	TC	TW	YL	ALL
n	53	48	54	54	50	52	311
Ammonium Sulfate (blue dots)							
Slope	1.011 (± 0.020)	1.018 (± 0.020)	1.107 (± 0.029)	1.093 (± 0.023)	1.065 (± 0.018)	1.074 (± 0.022)	1.055 (± 0.009)
Intercept	0.467 (± 0.088)	0.345 (± 0.087)	0.232 (± 0.101)	0.147 (± 0.094)	0.247 (± 0.073)	0.240 (± 0.092)	0.295 (± 0.037)
R^2	0.980	0.983	0.967	0.977	0.987	0.980	0.978
AVG Mea. NH_4^+	3.682	3.846	3.128	3.503	3.403	3.556	3.514
AVG Cal. NH_4^+	4.189	4.259	3.696	3.977	3.871	4.058	4.004
AVG Cal./Mea. NH_4^+	1.182 (± 0.120)	1.131 (± 0.082)	1.212 (± 0.147)	1.152 (± 0.108)	1.206 (± 0.380)	1.198 (± 0.296)	1.181 (± 0.217)
Ammonium Bisulfate (brown dots)							
Slope	0.530 (± 0.014)	0.533 (± 0.017)	0.558 (± 0.016)	0.566 (± 0.016)	0.553 (± 0.012)	0.591 (± 0.021)	0.556 (± 0.007)
Intercept	0.353 (± 0.061)	0.294 (± 0.073)	0.194 (± 0.057)	0.153 (± 0.064)	0.219 (± 0.048)	0.155 (± 0.088)	0.225 (± 0.027)
R^2	0.965	0.958	0.959	0.960	0.979	0.941	0.958
AVG Mea. NH_4^+	3.682	3.846	3.128	3.503	3.403	3.556	3.514
AVG Cal. NH_4^+	2.306	2.343	1.940	2.134	2.101	2.256	2.177
AVG Cal./Mea. NH_4^+	0.660 (± 0.083)	0.630 (± 0.066)	0.644 (± 0.091)	0.623 (± 0.073)	0.667 (± 0.242)	0.671 (± 0.190)	0.649 (± 0.140)

3.3.3 Charge Balance

For the anion and cation balance, the sum of Cl^-, NO_3^-, and SO_4^{2-} is compared to the sum of NH_4^+, Na^+, and K^+ in μeq/m^3 using the following equations:

$$\mu eq/m^3 \text{ for anions } = \left(\frac{Cl^-}{35.453} + \frac{NO_3^-}{62.005} + \frac{SO_4^{2-}}{98/2} \right)$$

$$\mu eq/m^3 \text{ for cations } = \left(\frac{NH_4^+}{18.04} + \frac{Na^+}{23.0} + \frac{K^+}{39.098} \right)$$

The cation equivalents are plotted against the anion equivalents in Figure 7. A strong correlation (R^2 = 0.98) was observed for the $PM_{2.5}$ samples collected at all of the sampling sites. The slopes are expected to be slightly larger than unity since the calculations only accounted for major measured ions and there is a deficiency in cations due to the exclusion of [H^+], [Ca^{2+}], and [Mg^{2+}]. Seen from the figure, the slopes obtained from individual sites range from 0.91 to 1.00. The difference is most likely caused by the underestimation of chloride and nitrate measurements on QMA filters.

The outliers are circled in Figure 7, including the following samples: MK120821, CW120821, WB120821, TC120827, TW120815, TW120821, TW120827, YL120815 and YL120827. A closer examination in these data points showed that the higher NO_3^- concentration is the culprit causing the anion-cation imbalance. It was also found in these samples that the water-soluble Ca^{2+} concentrations were abnormally high. Table 15 summarized the NO_3^- and soluble Ca^{2+} concentrations together with the total Ca concentrations (by XRF analysis) for comparison for the captioned samples. A fairly good correlation between the NO_3^- concentration vs. the "extra" calcium which was calculated as the difference between soluble Ca^{2+} and the total Ca (Figure 8) suggests that these filter samples might be contaminated. Since these samples were analyzed in the 3rd batch IC analysis in which there were a total of 120 filter samples and the rest of the samples remained normal. It is suspected that the $Ca(NO_3)_2$ contamination might occur during the pre- or/and post-sampling filter handling.

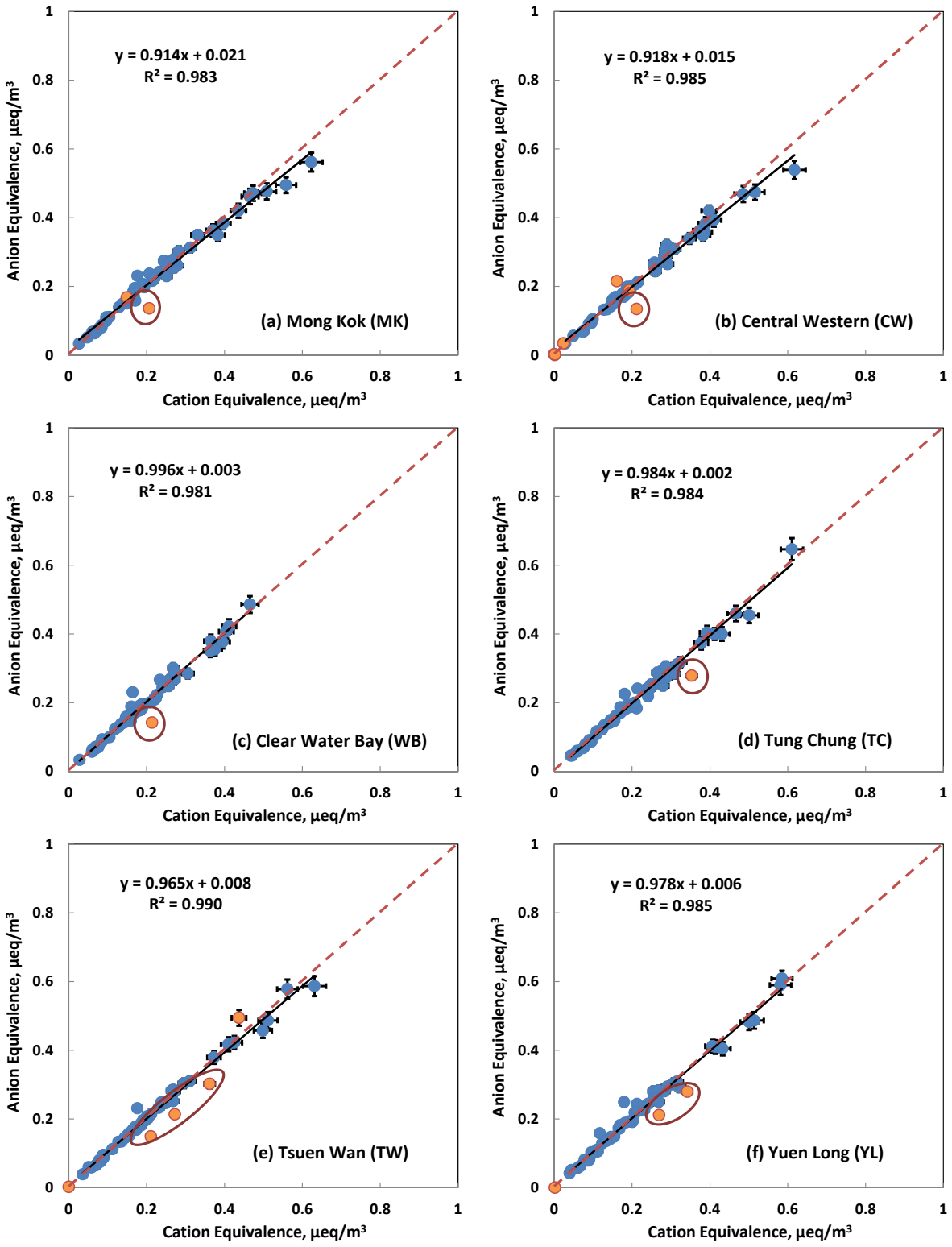

Figure 7. Scatter plots of anion versus cation measurements for $PM_{2.5}$ samples collected at (a) MK, (b) CW, (c) WB, (d) TC, (e) TW, and (f) YL.

Table 14. Statistics analysis of anion versus cation measurements for $PM_{2.5}$ samples collected at individual sites.

Statistics/Site	MK	CW	WB	TC	TW	YL	ALL
n	53	48	54	54	50	52	311
Slope	0.914 (± 0.017)	0.918 (± 0.016)	0.996 (± 0.019)	0.984 (± 0.018)	0.965 (± 0.014)	0.978 (± 0.017)	0.956 (± 0.007)
Intercept	0.021 (± 0.004)	0.015 (± 0.004)	0.003 (± 0.004)	0.002 (± 0.004)	0.008 (± 0.003)	0.006 (± 0.004)	0.010 (± 0.002)
R^2	0.983	0.985	0.981	0.984	0.990	0.985	0.984
AVG Σcation	0.227	0.237	0.198	0.218	0.210	0.221	0.218
AVG Σanion	0.229	0.233	0.201	0.216	0.211	0.222	0.218
AVG Σanion/Σcation	1.030 (± 0.083)	0.997 (± 0.062)	1.018 (± 0.079)	0.995 (± 0.064)	1.011 (± 0.063)	1.016 (± 0.090)	1.011 (± 0.075)

Table 15. Concentrations of total Ca, water-soluble Ca^{2+} and NO_3^- for outlier samples in Figure 7.

Sample ID	Filter ID	Conc. of Ca, μg/m^3	Sample ID	Filter ID	Conc. of Ca^{2+}, μg/m^3	Conc., of NO_3^-, μg/m^3
MK120821ST01T	T0000405	0.0954	MK120821SQ01Q	Q0000411	2.515	1.303
CW120821ST02T	T0000407	0.0695	CW120821SQ02Q	Q0000412	2.965	1.285
WB120821ST03T	T0000409	0.0664	WB120821SQ03Q	Q0000413	2.981	1.129
			WB120821SC03Q	Q0000414	2.889	1.274
WB120827ST03T	T0000417	0.1180	WB120827SC03Q	Q0000422	3.157	2.060
TC120827ST04T	T0000418	0.1180	TC120827SQ04Q	Q0000423	3.076	1.533
			TC120827SC04Q	Q0000424	3.158	1.514
TW120815ST05T	T0000403	0.0790	TW120815SQ05Q	Q0000409	3.272	2.356
TW120821ST05T	T0000411	0.4671	TW120821SQ05Q	Q0000417	3.654	1.274
TW120827ST05T	T0000419	0.1649	TW120827SQ05Q	Q0000425	3.341	2.414
YL120815ST06T	T0000404	0.0738	YL120815SQ06Q	Q0000410	3.598	2.961
YL120827ST06T	T0000420	0.1668	YL120827SQ06Q	Q0000426	3.222	2.165

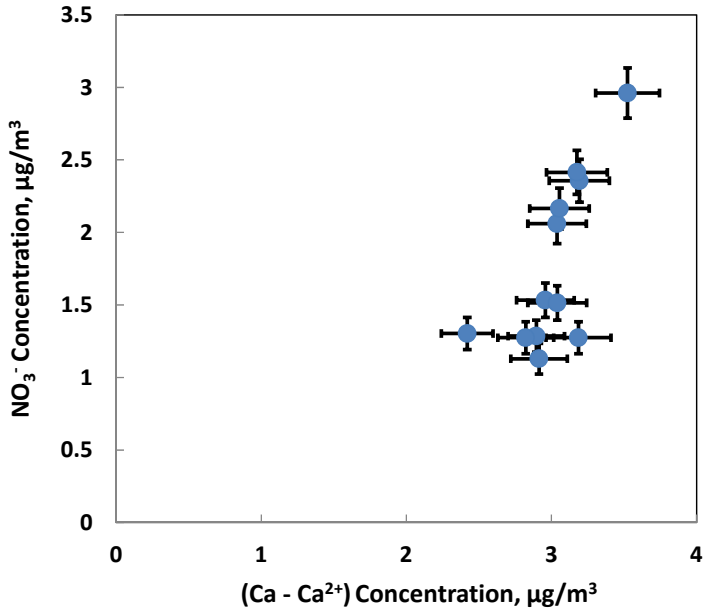

Figure 8. Scatter plot of NO_3^- vs. "extra" Ca (total Ca by XRF - soluble Ca^{2+} by IC) for the outlier samples observed in Figure 7.

3.3.4 NIOSH_TOT versus IMPROVE_TOR for Carbon Measurements

Carbon concentrations were determined for the collected $PM_{2.5}$ samples by both NIOSH_TOT and IMPROVE_TOR methods. The total carbon (TC) concentrations obtained from NIOSH_TOT and IMPROVE_TOR reach an excellent agreement (Figure 9), giving credence to the validities of the analysis results from both methods. The comparison results of OC and EC determined by both methods for individual sites are shown in Figure 10. Generally, EC concentrations derived by NIOSH_TOT method were much lower than those by IMPROVE_TOR method. The difference in EC obtained by these two protocols has been well-documented and is primarily a result of protocol-dependent nature of correction of charring of OC formed during thermal analysis [e.g., *Chow et al.*,2004; *Chen et al.*, 2004; *Subraminan et al.*, 2006]. Seen from the results, the average ratios of NIOSH_TOT EC to IMPROVE_TOR EC for samples from individual sampling sites range from 0.41 ± 0.10 at WB to 0.63 ± 0.18 at MK (Table 16). No correlation was found between NIOSH_TOT EC and IMPROVE_TOR EC for samples collected at Mong Kok site, which have very high EC loading on the QMA filters.

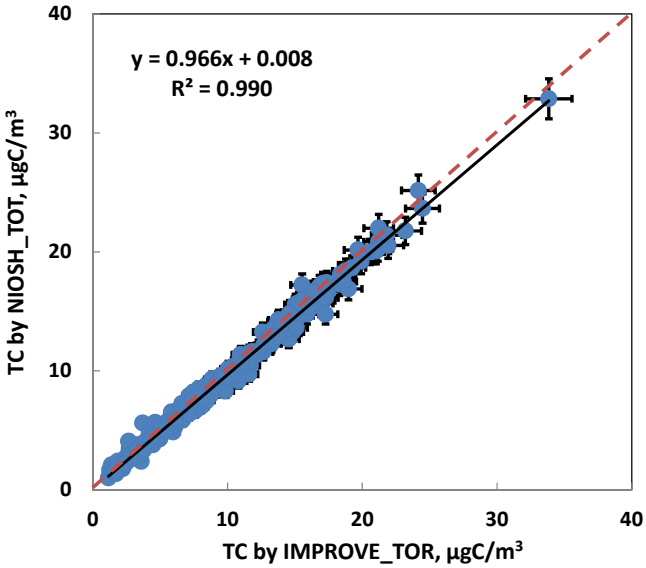

Figure 9. Comparisons of TC determined by NIOSH_TOT and IMPROVE_TOR methods for $PM_{2.5}$ samples collected at all sites.

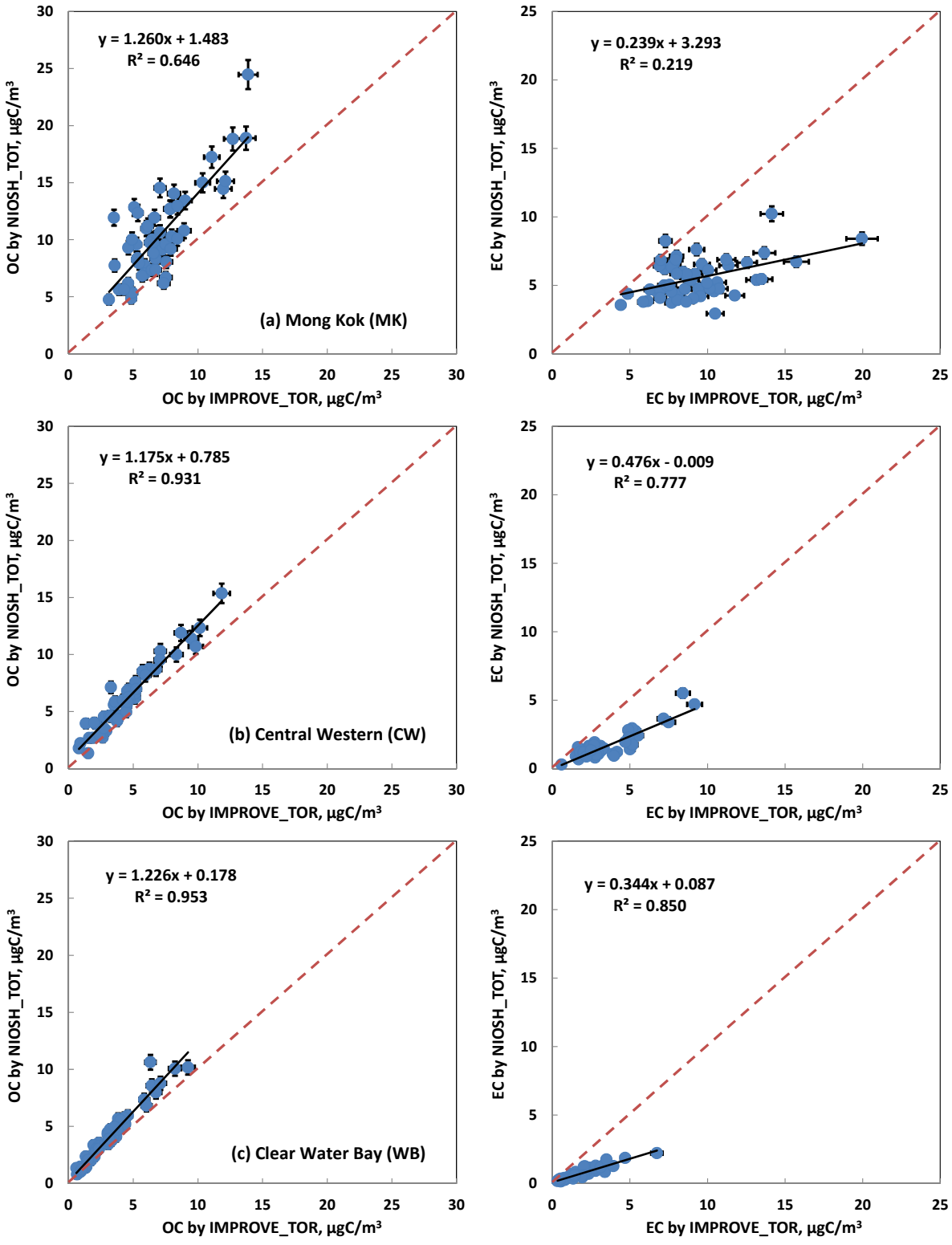
y = 1.260x + 1.483
R² = 0.646
(a) Mong Kok (MK)
OC by NIOSH_TOT, µgC/m³
OC by IMPROVE_TOR, µgC/m³
y = 0.239x + 3.293
R² = 0.219
EC by NIOSH_TOT, µgC/m³
EC by IMPROVE_TOR, µgC/m³
y = 1.175x + 0.785
R² = 0.931
(b) Central Western (CW)
y = 0.476x - 0.009
R² = 0.777
y = 1.226x + 0.178
R² = 0.953
(c) Clear Water Bay (WB)
y = 0.344x + 0.087
R² = 0.850

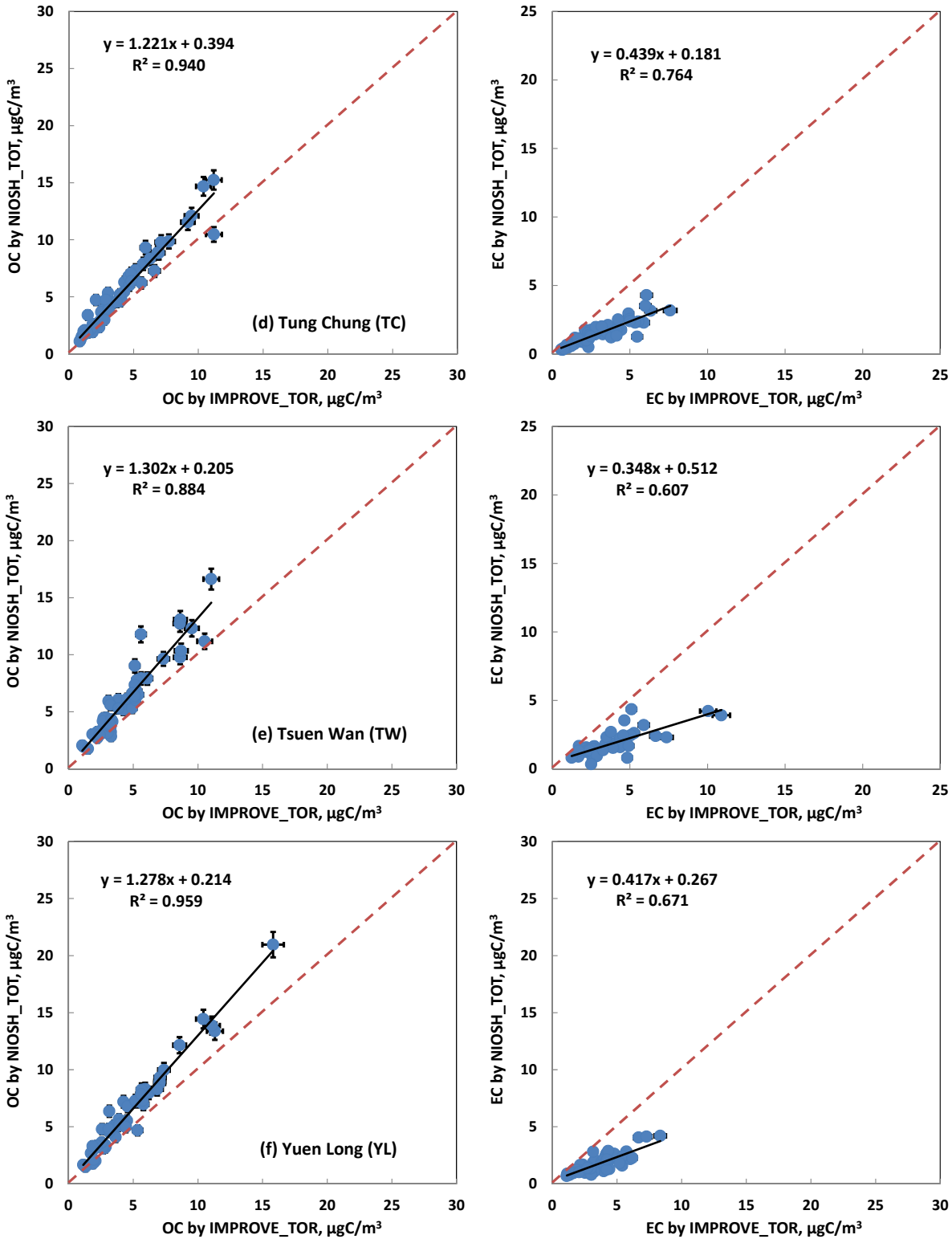

Figure 10. Comparisons of OC and EC determined by NIOSH_TOT and IMPROVE_TOR methods for $PM_{2.5}$ samples collected at (a) MK, (b) CW, (c) WB, (d) TC, (e) TW, and (f) YL.

Table 16. Statistics analysis of OC and EC determined by NIOSH_TOT and IMPROVE_TOR methods for $PM_{2.5}$ samples collected at individual sites.

Statistics/Site	MK	CW	WB	TC	TW	YL	ALL
n	53	48	54	54	50	52	311
NIOSH_TOT OC versus IMPROVE_TOR OC							
Slope	1.260 (± 0.131)	1.175 (± 0.047)	1.226 (± 0.038)	1.221 (± 0.043)	1.302 (± 0.068)	1.278 (± 0.037)	1.319 (± 0.027)
Intercept	1.483 (± 0.976)	0.785 (± 0.243)	0.178 (± 0.139)	0.394 (± 0.211)	0.205 (± 0.351)	0.214 (± 0.205)	0.207 (± 0.145)
R^2	0.646	0.931	0.953	0.940	0.884	0.959	0.888
AVG TOR_OC	7.055	4.492	3.072	4.136	4.567	4.689	4.666
AVG TOT_OC	10.370	6.064	3.944	5.445	6.150	6.207	6.360
AVG TOT_OC/TOR_OC	1.510 (± 0.438)	1.434 (± 0.383)	1.302 (± 0.208)	1.356 (± 0.248)	1.365 (± 0.250)	1.337 (± 0.215)	1.383 (± 0.308)
NIOSH_TOT EC versus IMPROVE_TOR EC							
Slope	0.239 (± 0.063)	0.476 (± 0.038)	0.344 (± 0.020)	0.439 (± 0.034)	0.348 (± 0.040)	0.417 (± 0.041)	0.534 (± 0.015)
Intercept	3.293 (± 0.606)	-0.009 (± 0.149)	0.087 (± 0.044)	0.181 (± 0.119)	0.512 (± 0.165)	0.267 (± 0.163)	-0.051 (± 0.078)
R^2	0.219	0.777	0.850	0.764	0.607	0.671	0.800
AVG TOR_EC	9.199	3.518	1.843	3.072	3.593	3.604	4.144
AVG TOT_EC	5.491	1.664	0.721	1.528	1.762	1.768	2.162
AVG TOT_EC/TOR_EC	0.626 (± 0.176)	0.489 (± 0.143)	0.411 (± 0.103)	0.517 (± 0.126)	0.523 (± 0.166)	0.515 (± 0.141)	0.514 (± 0.157)

3.3.5 Material Balance

Major PM components can be classified into seven categories including: 1) geological material, which can be estimated by (1.89 × [Al] + 2.14 × [Si] + 1.4 × [Ca] + 1.43 × [Fe]); 2) organic matter, which can be estimated from OC concentration as [OM] = 1.4 × [OC]; 3) soot which can be represented by EC concentration; 4) ammonium sulfate (1.38 × [SO_4^{2-}]); 5) ammonium nitrate (1.29 × [NO_3^-]); 6) non-crustal trace elements; 7) Unidentified material. Considering the large uncertainty in Na measurement by XRF, soluble sodium is used in calculation instead of total sodium. Therefore, the reconstructed mass is calculated by the following equation,

[Reconstructed Mass]

= 1.89 × [Al] + 2.14 × [Si] + 1.4 × [Ca] + 1.43 × [Fe]

\+ 1.4 × [OC]

\+ [EC]

\+ 1.38 × [SO_4^{2-}]

\+ 1.29 × [NO_3^-]

\+ [Na^+]

\+ trace elements excluding Na, Al, Si, Ca, Fe, and S

The reconstructed mass is plotting against the measured mass in Figure 11. A strong correlation (R^2 = 0.98) is observed between the reconstructed mass and measured mass with a slope of 0.91 ± 0.01. Different from the comparison made between sum of chemical species and measured mass (Figure 2), the major uncertainty of the reconstructed mass is due to the estimation of organic matter (OM). Generally, the concentration of OM is determined by multiplying the OC concentration by an empirical factor. In this study, a value of 1.4 was applied to this factor. It is worth noting that the [OM]/[OC] ratio is site dependent. The [OM]/[OC] ratio of freshly emitted aerosols is smaller than that of the more aging (oxygenated) aerosols. Since a constant conversion factor is adopted for calculation in this study, it can be seen that the average ratio of reconstructed mass to measured mass has the highest value for MK site, which is a roadside station and the dominant air mass is more freshly generated.

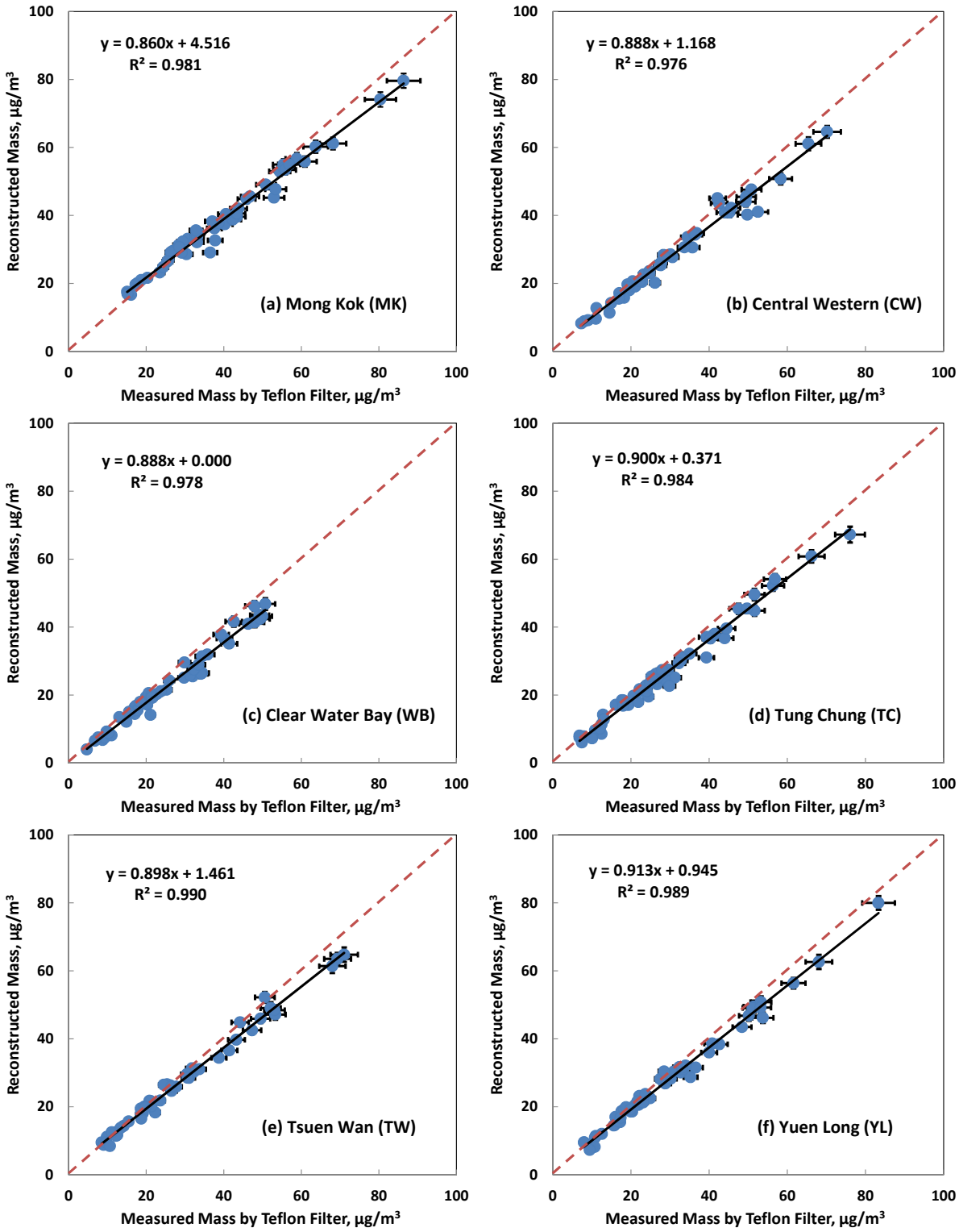

Figure 11. Scatter plots of reconstructed mass versus measured mass on Teflon filters for $PM_{2.5}$ samples collected at (a) MK, (b) CW, (c) WB, (d) TC, (e) TW, and (f) YL.

Table 17. Statistics analysis of reconstructed mass versus measured mass on Teflon filters for $PM_{2.5}$ samples collected at individual sites.

Statistics/Site	MK	CW	WB	TC	TW	YL	ALL
n	53	48	54	54	50	52	311
Slope	0.860 (± 0.017)	0.888 (± 0.021)	0.888 (± 0.019)	0.900 (± 0.016)	0.898 (± 0.013)	0.913 (± 0.013)	0.908 (± 0.007)
Intercept	4.516 (± 0.708)	1.168 (± 0.704)	0.000 (± 0.530)	0.371 (± 0.524)	1.461 (± 0.440)	0.945 (± 0.459)	0.856 (± 0.254)
R^2	0.981	0.976	0.978	0.984	0.990	0.989	0.980
AVG Mea. Mass	38.934	30.866	25.482	29.070	28.644	30.153	30.518
AVG Rec. Mass	38.008	28.565	22.622	26.523	27.190	28.473	28.552
AVG Rec./Mea. Mass	0.998 (± 0.080)	0.938 (± 0.077)	0.888 (± 0.074)	0.919 (± 0.090)	0.965 (± 0.071)	0.956 (± 0.079)	0.944 (± 0.086)

The annual average composition (%) of the major components to the $PM_{2.5}$ mass is shown in Figure 12 for individual sites. The unidentified mass for MK, CW, WB, TC, TW, and YL is 2.8%, 7.7%, 12.3%, 9.2%, 5.6%, and 6.0% of the measured mass, respectively. Overall, the reconstructed mass agrees with the measured mass within approx. 7%.

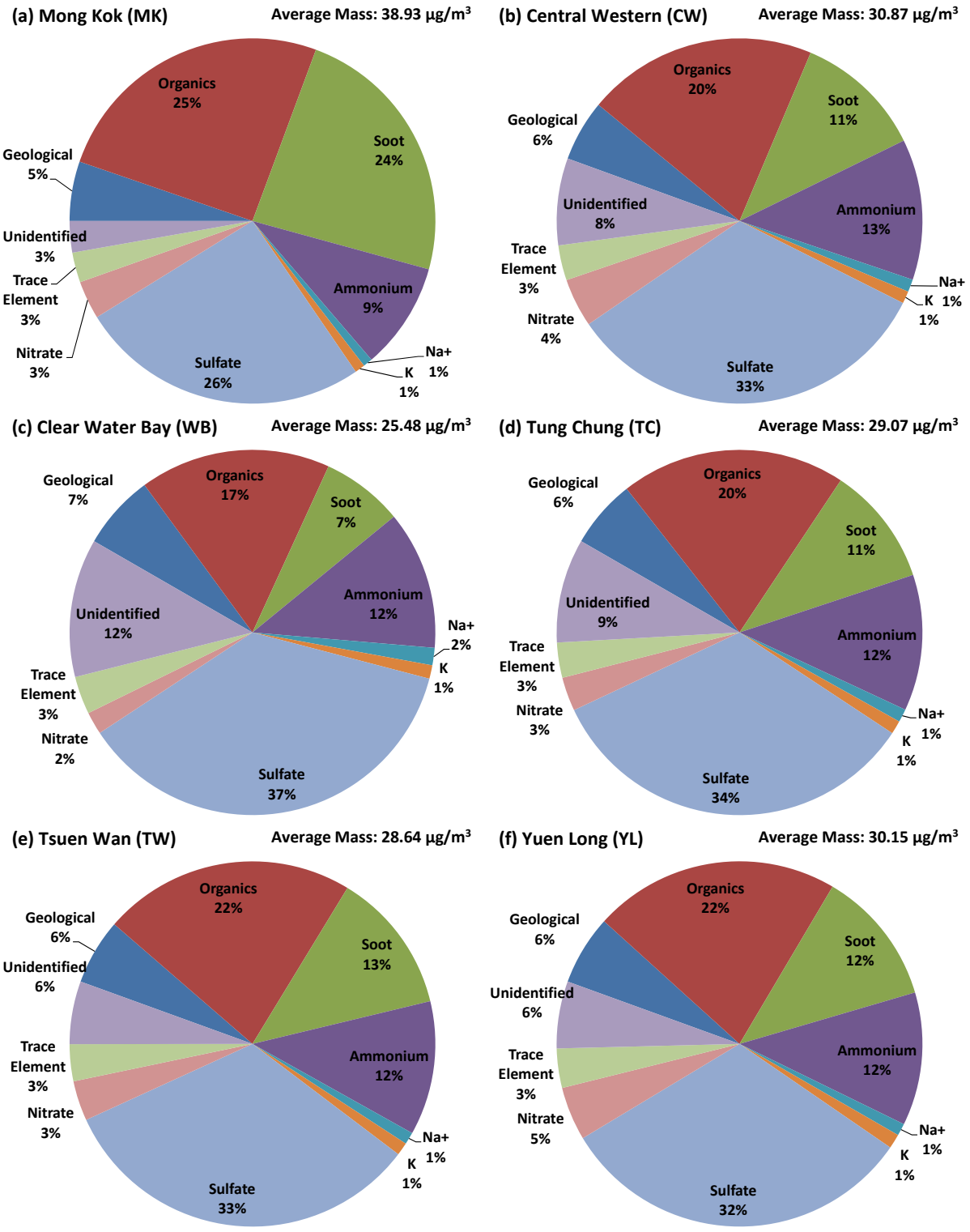

Figure 12. Annual average composition (%) of major components including 1) geological material; 2) organic matter; 3) soot; 4) ammonium; 5) sulfate; 6) nitrate; 7) non-crustal trace elements, and 8) Unidentified material (difference between measured mass and the reconstructed mass) to $PM_{2.5}$ mass for (a) MK, (b) CW, (c) WB, (d) TC, (e) TW, and (f) YL.

Annually MK had the highest $PM_{2.5}$ loading while WB had the lowest (Figure 13). For all of the six sites, sulfate and OM were two most abundant components followed by ammonium and soot (EC by IMPROVE_TOR method). The EC concentration was the highest at MK and the lowest at WB, which is consistent with the natures of the sampling sites. The concentrations of sulfate, ammonium, geological materials, and trace elements didn't vary much across all six sites.

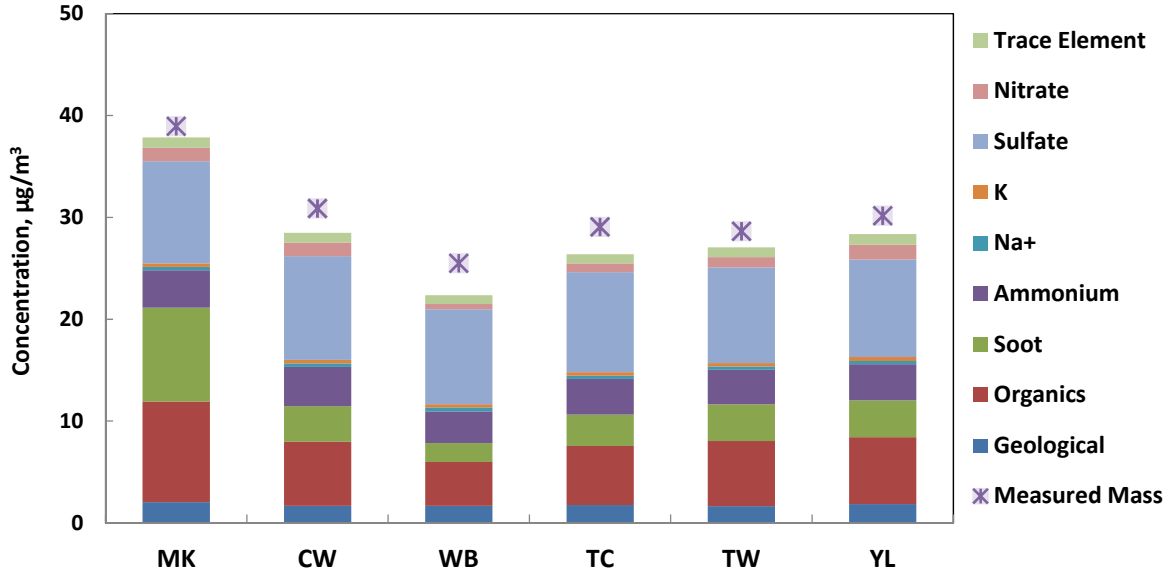

Figure 13. Comparison of annual average concentrations of major components including 1) geological material; 2) organic matter; 3) soot; 4) ammonium; 5) sulfate; 6) nitrate; 7) non-crustal trace elements, and 8) Unidentified material (difference between measured mass and the reconstructed mass) to $PM_{2.5}$ mass between individual sites.

3.3.6 Comparison of Collocated Samples

Collocated samplings were conducted in MK and CW sites on Teflon filters, and in WB and TC sites on QMA filters. The comparison of the collocated samples serves as part of the quality assurance efforts for the PM study with the purpose of determining the reproducibility of the sampling and analytical methods.

The data used for this comparison were subject to a data screening procedure including two steps. First, species that can be quantified (concentration > LOQ) more than 70% of the time will be included. Second, if either of the values in one pair of samples is below the LOQ, the whole pair of samples will be removed from the data set.

Bias and precisions were computed for collocated comparisons on $PM_{2.5}$ and selected chemical species with the screened data set. The equations used are as below,

$$\overline{C_i} = \frac{X_i + Y_i}{2} \quad (10)$$

$$\%RB_i = \frac{(Y_i - X_i)}{\overline{C_i}} \times 100\% \quad (11)$$

$$\%\overline{RB} = \frac{1}{n}\sum_{i=1}^{n} \frac{(Y_i - X_i) \times 100\%}{\overline{C_i}} \quad (12)$$

$$\%RSD = \frac{|\%RB_i|}{\sqrt{2}} \quad (13)$$

$$\%\overline{RSD} = \sqrt{\frac{1}{n}\sum_{i=1}^{n} \%RSD_i^2} \quad (14)$$

where:

X_i = ambient air concentration of sample i measured at sampler X, µg/m^3

Y_i = ambient air concentration of sample i measured at collocated sampler Y, µg/m^3

n = number of paired samples

%RB = percent relative bias

%RSD = percent relative standard deviation

The method for comparison used in this analysis gives a measure of the overall precision of the PM study, i.e. the sampling stage and the analytical stage are combined. The results (Table 18) show that the average relative biases of the concentrations of $PM_{2.5}$ and selected chemical species for collocated samples are below 10%. It suggests that the precision of the PM sampling/analytical methods are acceptable.

Table 18. Average relative biases and average relative standard deviations of concentrations of $PM_{2.5}$ and selected chemical species for collocated samples.

	No. of Paired Samples	Average Relative Bias (%RB)	Average Relative Standard Deviation (%RSD)
$PM_{2.5}$_Teflon	107	-3.14	13.89
$PM_{2.5}$_QMA	110	-0.04	15.42
Na^+	96	0.55	10.26
NH_4^+	107	-0.71	5.57
K^+	98	-2.40	10.01
NO_3^-	104	7.17	16.11
SO_4^{2-}	107	-1.21	5.52
TOR_OC	107	0.42	7.39
TOR_EC	107	0.40	6.84
Al	107	0.62	6.39
Si	103	1.77	6.51
S	107	0.09	3.44
K	107	0.34	3.55
Ca	107	1.72	5.84
Ti	105	0.84	16.40
V	107	-0.83	7.97
Fe	107	2.42	5.15
Cu	107	2.04	8.43
Zn	106	1.02	5.12

3.3.7 $PM_{2.5}$ Mass Concentrations: Gravimetric vs. Continuous Measurements

Continuous monitoring of $PM_{2.5}$ concentrations by TEOMs (tapered element oscillating microbalance) is carried out at a few locations in Hong Kong, including in MK, CW, TC, TW, and YL sites. A beta gauge particulate monitor (Model 5030 SHARP, Thermo Scientific) has been set up in HKUST site for continuous monitoring of $PM_{2.5}$ concentrations since May 2011. Comparisons of $PM_{2.5}$ mass concentrations from gravimetric measurement and 24-hr average TEOM/beta gauge measurement were conducted. The results are presented in both time-series plots and scatter plots (Figure 14). Uncertainties of TEOM/beta gauge are assumed to be 5% of concentration. The two measurements show good agreement (R^2 = 0.87 - 0.97) with slopes ranging from 0.97 to 1.18.

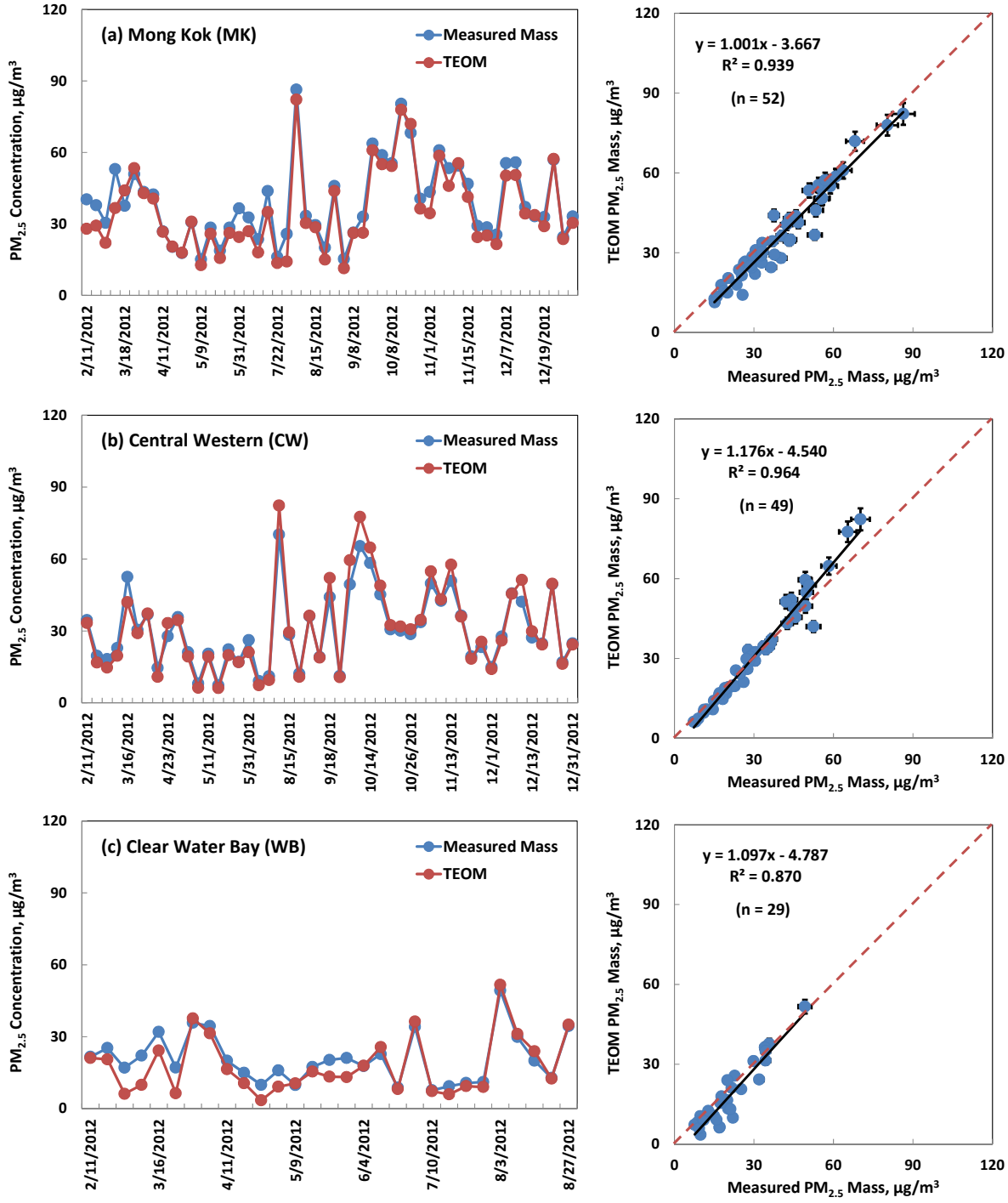

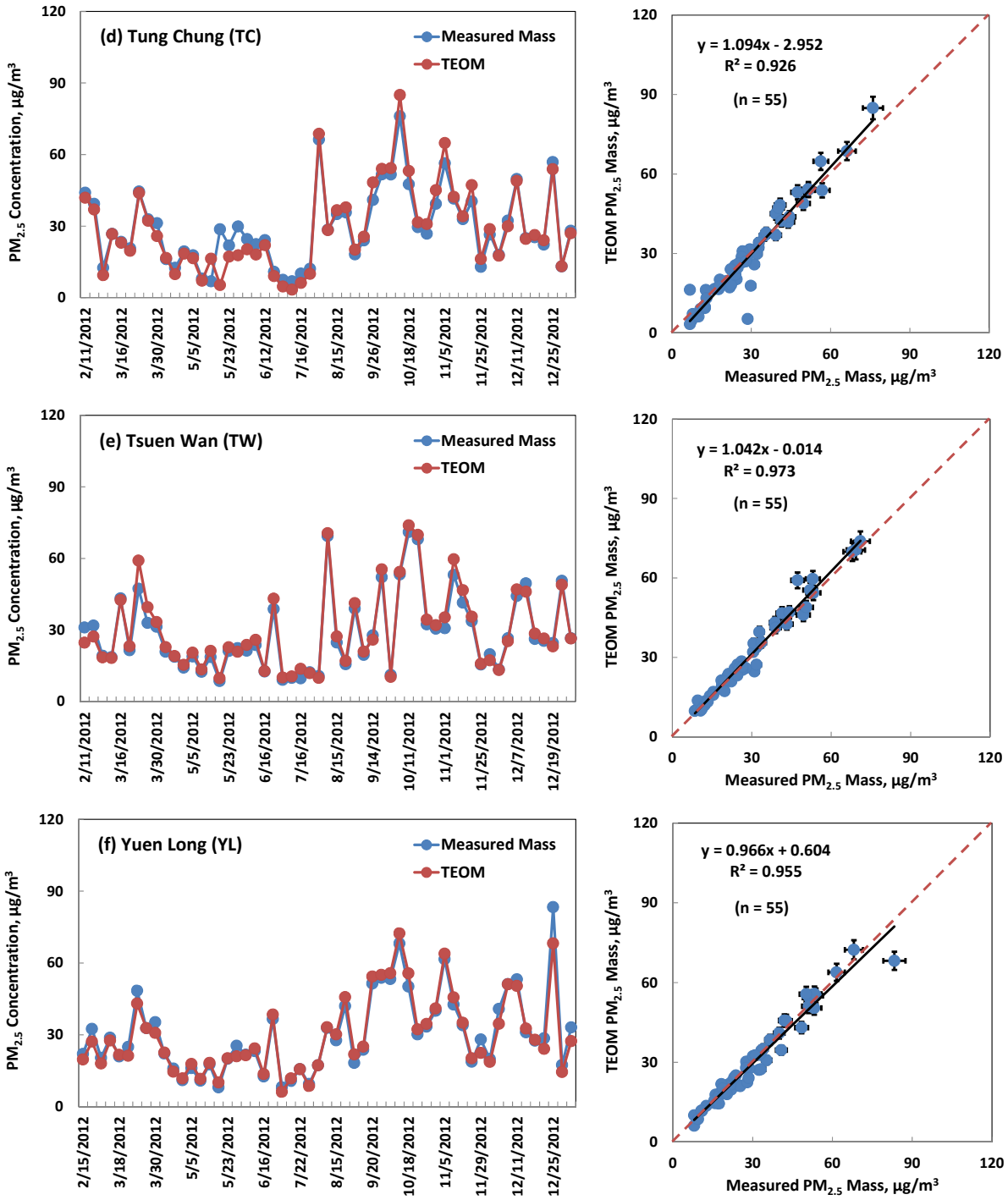

Figure 14. Comparisons of $PM_{2.5}$ mass concentrations from gravimetric and continuous measurements at (a) MK, (b) CW, (c) WB, (d) TC, (e) TW, and (f) YL.

4. Comparison to the $PM_{2.5}$ Sampling Campaigns in 2000 - 2001, 2004 - 2005, 2008 - 2009 and 2011

A side-by-side comparison of the five year study of $PM_{2.5}$ samples collected during 2000 - 2001, 2004 - 2005, the whole year of 2009, the whole year of 2011, and the current 2012 period is shown in Table 19 [*Chow et al.*, 2002, 2006, 2010; *Yu et al.*, 2012]. In this study, the $PM_{2.5}$ monitoring sites remained the same as those in the year of 2011.

Compared to the year of 2011, the annual average $PM_{2.5}$ concentrations of 2012 exhibited a decrease of 10.4%, 13.8%, 19.4%, 17.9%, 19.1% and 20.7% at MK, CW, WB, TC, TW and YL sites, respectively. In particular, MK, TW, and YL sites were picked out for annual trend observation. The annual average $PM_{2.5}$ concentrations recorded at these three sites were all found to decrease from 2005 to 2009, slightly increased in 2011 and then decrease again in current study (Figure 15).

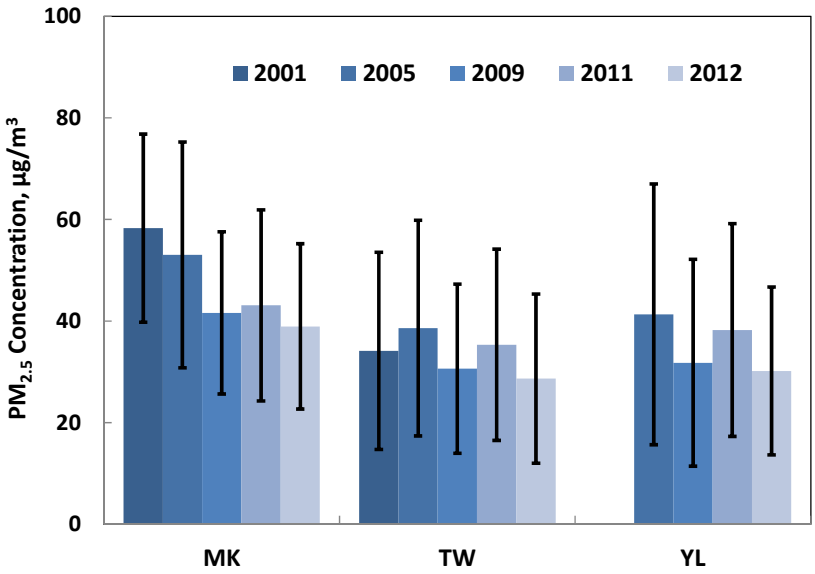

Figure 15. Comparisons of annual average $PM_{2.5}$ mass concentrations at MK, TW, and YL sites from 2001 to 2012. The error bars represent one standard variation of the $PM_{2.5}$ mass concentration measurements over the year.

Table 19. Side-by-side comparison of the four one-year studies of $PM_{2.5}$ samples (in µg/m3) collected during 2000 - 2001, 2004 - 2005, 2008 - 2009, 2011 and current 2012 (2/2012 - 12/2012) period. Carbon concentrations are from the IMPROVE_TOR method.

	2001 MK	2001 TW	2001 HT	2005 MK	2005 TW	2005 YL	2005 HT	2009 MK	2009 TW	2009 YL	2009 HT	2011 MK	2011 CW	2011 WB	2011 TC	2011 TW	2011 YL	2012 MK	2012 CW	2012 WB	2012 TC	2012 TW	2012 YL
Teflon Mass	58.281	34.122	23.658	53.023	38.593	41.310	28.437	41.600	30.612	31.781	24.105	43.077	35.364	31.320	35.572	35.298	38.220	38.934	30.866	25.482	29.070	28.644	30.153
Quartz Mass	62.502	37.280	25.848	54.868	40.748	43.908	29.643	45.924	34.003	36.343	25.945	47.922	39.841	35.893	39.811	40.558	42.895	58.035	49.444	45.577	46.958	48.255	50.229
Cl-	0.256	0.138	0.143	0.283	0.126	0.264	0.124	0.312	0.175	0.213	0.298	0.205	0.191	0.105	0.109	0.122	0.174	0.102	0.116	0.067	0.072	0.082	0.131
NO3-	1.653	1.343	0.708	2.404	1.635	2.864	0.762	2.809	2.031	2.419	1.508	2.452	2.389	0.934	1.897	1.795	2.590	1.321	1.329	0.508	0.868	1.015	1.434
SO4=	9.502	9.172	8.641	12.840	13.174	13.910	11.906	10.414	10.481	11.041	9.657	10.912	10.907	11.128	11.094	10.914	10.851	10.015	10.194	9.338	9.804	9.411	9.583
NH4+	3.174	2.965	2.157	4.400	4.070	4.617	3.059	3.402	3.268	3.470	2.631	4.373	4.454	4.090	4.377	4.385	4.627	3.682	3.846	3.128	3.503	3.403	3.556
Na+	0.398	0.397	0.679	0.423	0.362	0.375	0.527	0.320	0.211	0.262	0.380	0.431	0.452	0.510	0.413	0.404	0.402	0.324	0.344	0.394	0.338	0.306	0.323
K+	0.457	0.492	0.403	0.479	0.486	0.562	0.433	0.278	0.308	0.365	0.259	0.467	0.463	0.483	0.534	0.492	0.590	0.349	0.344	0.288	0.344	0.318	0.374
OC	16.642	8.690	4.226	11.177	6.932	7.235	3.921	6.262	4.376	4.834	2.697	8.094	4.918	3.905	5.125	5.435	5.727	7.055	4.492	3.072	4.136	4.567	4.689
EC	20.288	5.371	1.682	14.115	6.258	6.194	2.277	10.661	3.760	3.488	1.206	8.481	3.709	2.431	3.654	4.238	4.606	9.199	3.518	1.843	3.072	3.593	3.604
TC	36.911	14.041	5.890	25.284	13.181	13.420	6.190	16.912	8.124	8.310	3.892	16.550	8.604	6.313	8.756	9.649	10.309	16.254	8.009	4.915	7.208	8.160	8.294
Al	0.1139	0.1146	0.1094	0.1408	0.1414	0.1448	0.1223	0.0986	0.0828	0.0913	0.0828	0.1942	0.2008	0.1990	0.2009	0.1910	0.2114	0.2365	0.2134	0.2260	0.2322	0.212	0.2368
Si	0.4778	0.3870	0.3489	0.3469	0.3141	0.3221	0.2546	0.2485	0.1853	0.2073	0.1685	0.3981	0.4209	0.3980	0.4079	0.3888	0.4349	0.4393	0.3882	0.4064	0.4175	0.3899	0.4311
P	0.0092	0.0050	0.0028	0.1886	0.1950	0.1917	0.1747	0.0225	0.0237	0.0229	0.0225	0.0194	0.0163	0.0150	0.0158	0.0163	0.0155	0.0211	0.0144	0.0129	0.0140	0.0138	0.0148
S	3.4886	3.3789	3.0534	4.3005	4.5835	4.5622	4.2099	3.3471	3.4305	3.4535	3.1650	3.6677	3.7263	3.8399	3.7518	3.7641	3.7813	3.3455	3.4259	3.1763	3.3431	3.1509	3.2280
Cl	0.1169	0.0874	0.1432	0.1391	0.0758	0.1590	0.0709	0.1037	0.0568	0.0941	0.0799	0.0889	0.1203	0.0720	0.0726	0.0640	0.0774	0.0386	0.0566	0.0235	0.0373	0.0491	0.0621
K	0.5517	0.5858	0.4892	0.4678	0.5080	0.5631	0.4551	0.3064	0.3281	0.3828	0.2780	0.4619	0.4677	0.4740	0.5192	0.4797	0.5722	0.3447	0.3324	0.3005	0.3454	0.3211	0.3882
Ca	0.1705	0.1262	0.1024	0.1082	0.0896	0.0891	0.0652	0.1102	0.0729	0.0738	0.0626	0.1298	0.1209	0.0914	0.0959	0.1006	0.1111	0.1461	0.1072	0.1090	0.1117	0.1253	0.1207
Ti	0.0092	0.0088	0.0079	0.0109	0.0102	0.0114	0.0062	0.0109	0.0084	0.0097	0.0062	0.0128	0.0118	0.0106	0.0138	0.0117	0.0156	0.0147	0.0124	0.0116	0.0147	0.0127	0.0153
V	0.0134	0.0137	0.0117	0.0190	0.0237	0.0195	0.0167	0.0175	0.0182	0.0144	0.0177	0.0146	0.0150	0.0119	0.0139	0.0206	0.0139	0.0197	0.0182	0.0133	0.0140	0.0208	0.0145
Cr	0.0010	0.0009	0.0006	0.0017	0.0015	0.0017	0.0014	0.0014	0.0012	0.0016	0.0011	0.0021	0.0020	0.0022	0.0022	0.0021	0.0024	0.0023	0.0022	0.0019	0.0022	0.0022	0.0022
Mn	0.0128	0.0124	0.0077	0.0170	0.0158	0.0170	0.0123	0.0127	0.0113	0.0127	0.0087	0.0214	0.0214	0.0174	0.0226	0.0186	0.0215	0.0194	0.0168	0.0132	0.0158	0.0163	0.0190
Fe	0.2692	0.1871	0.1219	0.2579	0.1858	0.1996	0.1190	0.2343	0.1325	0.1552	0.0947	0.2958	0.1978	0.1582	0.2094	0.1932	0.2215	0.3051	0.1881	0.1527	0.1959	0.1962	0.2223
Co	0.0001	0.0001	0.0002	0.0001	0.0001	0.0001	0.0002	0.0002	0.0002	0.0001	0.0002	0.0005	0.0005	0.0003	0.0004	0.0003	0.0004	0.0002	0.0001	0.0001	0.0001	0.0001	0.0001
Ni	0.0055	0.0054	0.0047	0.0061	0.0071	0.0068	0.0050	0.0049	0.0052	0.0044	0.0050	0.0050	0.0050	0.0042	0.0048	0.0064	0.0049	0.0065	0.0060	0.0045	0.0048	0.0113	0.0051
Cu	0.0113	0.0090	0.0052	0.0110	0.0104	0.0113	0.0065	0.0210	0.0188	0.0167	0.0169	0.0252	0.0215	0.0225	0.0226	0.0207	0.0234	0.0214	0.0181	0.0177	0.0157	0.0151	0.0167
Zn	0.1794	0.1743	0.1087	0.2399	0.2186	0.2381	0.1727	0.1579	0.1343	0.1600	0.1177	0.2156	0.2364	0.1948	0.2909	0.1936	0.2188	0.1887	0.1598	0.1337	0.1366	0.1704	0.1879
Ga	0.0004	0.0004	0.0005	0.0018	0.0030	0.0024	0.0026	0.0003	0.0004	0.0003	0.0004	0.0003	0.0002	0.0002	0.0002	0.0001	0.0001	0.0001	0.0002	0.0002	0.0001	0.0000	0.0002
As	0.0046	0.0055	0.0042	0.0053	0.0063	0.0084	0.0043	0.0012	0.0010	0.0016	0.0006	0.0043	0.0046	0.0053	0.0050	0.0046	0.0058	0.0030	0.0036	0.0026	0.0032	0.0029	0.0029
Se	0.0021	0.0022	0.0020	0.0003	0.0004	0.0005	0.0004	0.0003	0.0004	0.0004	0.0006	0.0000	0.0000	0.0000	0.0000	0.0000	0.0000	0.0000	0.0000	0.0000	0.0000	0.0001	0.0000
Br	0.0129	0.0127	0.0121	0.0106	0.0099	0.0116	0.0108	0.0172	0.0148	0.0143	0.0174	0.0172	0.0170	0.0190	0.0159	0.0156	0.0171	0.0132	0.0134	0.0160	0.0115	0.0108	0.0122
Rb	0.0036	0.0043	0.0032	0.0020	0.0025	0.0029	0.0019	0.0010	0.0011	0.0015	0.0008	0.0011	0.0013	0.0014	0.0015	0.0014	0.0016	0.0007	0.0008	0.0006	0.0009	0.0006	0.0010
Sr	0.0013	0.0011	0.0011	0.0011	0.0011	0.0015	0.0015	0.0017	0.0019	0.0020	0.0015	0.0030	0.0032	0.0030	0.0027	0.0029	0.0030	0.0018	0.0015	0.0016	0.0016	0.0015	0.0014
Y	0.0001	0.0001	0.0002	0.0004	0.0004	0.0004	0.0003	0.0003	0.0004	0.0003	0.0004	0.0002	0.0002	0.0004	0.0002	0.0003	0.0004	0.0001	0.0001	0.0000	0.0001	0.0001	0.0001
Zr	0.0006	0.0006	0.0005	0.0016	0.0013	0.0007	0.0010	0.0010	0.0008	0.0011	0.0010	0.0006	0.0002	0.0003	0.0004	0.0004	0.0006	0.0014	0.0008	0.0006	0.0008	0.0005	0.0007
Mo	0.0005	0.0005	0.0007	0.0015	0.0011	0.0017	0.0012	0.0007	0.0006	0.0007	0.0005	0.0016	0.0012	0.0011	0.0011	0.0013	0.0009	0.0001	0.0000	0.0001	0.0001	0.0002	0.0001
Pd	0.0012	0.0017	0.0011	0.0019	0.0014	0.0016	0.0020	0.0006	0.0007	0.0008	0.0005	0.0016	0.0018	0.0023	0.0021	0.0019	0.0018	0.0000	0.0000	0.0000	0.0000	0.0000	0.0000
Ag	0.0011	0.0017	0.0014	0.0013	0.0020	0.0018	0.0012	0.0010	0.0007	0.0008	0.0007	0.0003	0.0002	0.0003	0.0002	0.0001	0.0001	0.0000	0.0006	0.0003	0.0003	0.0004	0.0002
Cd	0.0019	0.0023	0.0022	0.0022	0.0021	0.0025	0.0018	0.0008	0.0007	0.0007	0.0005	0.0006	0.0005	0.0005	0.0006	0.0004	0.0007	0.0007	0.0013	0.0007	0.0004	0.0010	0.0008
In	0.0018	0.0020	0.0014	0.0009	0.0010	0.0017	0.0011	0.0005	0.0005	0.0005	0.0005	0.0003	0.0003	0.0005	0.0006	0.0003	0.0002	0.0001	0.0000	0.0000	0.0000	0.0000	0.0001
Sn	0.0188	0.0203	0.0116	0.0131	0.0188	0.0162	0.0084	0.0107	0.0101	0.0100	0.0091	0.0131	0.0122	0.0125	0.0135	0.0120	0.0154	0.0041	0.0038	0.0035	0.0052	0.0032	0.0049
Sb	0.0046	0.0049	0.0038	0.0042	0.0027	0.0039	0.0033	0.0009	0.0009	0.0014	0.0015	0.0080	0.0074	0.0068	0.0075	0.0067	0.0087	0.0005	0.0005	0.0007	0.0007	0.0002	0.0004
Ba	0.0267	0.0170	0.0086	0.0106	0.0081	0.0068	0.0053	0.0031	0.0031	0.0024	0.0026	0.0167	0.0108	0.0087	0.0104	0.0101	0.0108	0.0348	0.0101	0.0127	0.0108	0.0115	0.0205
La	0.0131	0.0087	0.0130	0.0105	0.0081	0.0082	0.0112	0.0036	0.0034	0.0040	0.0053	0.0164	0.0156	0.0146	0.0163	0.0132	0.0165	0.0000	0.0000	0.0000	0.0000	0.0000	0.0000
Au	0.0003	0.0005	0.0004	0.0003	0.0006	0.0002	0.0003	0.0000	0.0000	0.0001	0.0002	0.0000	0.0000	0.0000	0.0000	0.0000	0.0000	0.0000	0.0002	0.0001	0.0002	0.0002	0.0001
Hg	0.0001	0.0002	0.0001	0.0000	0.0003	0.0001	0.0001	0.0000	0.0000	0.0000	0.0000	0.0000	0.0000	0.0000	0.0000	0.0000	0.0000	0.0000	0.0000	0.0000	0.0000	0.0000	0.0000
Tl	0.0001	0.0001	0.0001	0.0002	0.0001	0.0000	0.0003	0.0000	0.0001	0.0001	0.0000	0.0000	0.0000	0.0000	0.0000	0.0000	0.0000	0.0000	0.0000	0.0000	0.0000	0.0000	0.0000
Pb	0.0664	0.0726	0.0576	0.0478	0.0498	0.0624	0.0432	0.0405	0.0406	0.0437	0.0399	0.0597	0.0604	0.0626	0.0630	0.0599	0.0671	0.0399	0.0397	0.0370	0.0365	0.0346	0.0384
U	0.0001	0.0002	0.0002	0.0013	0.0011	0.0017	0.0018	0.0008	0.0007	0.0007	0.0010	0.0040	0.0035	0.0040	0.0038	0.0038	0.0035	0.0001	0.0000	0.0000	0.0000	0.0001	0.0000

Measured species were grouped into six categories described in Section 3.3.5 for better comparison (Figure 16).

At MK, TW and YL sites, the concentrations of ammonium and sulfate fluctuated among the years with the highest values observed in the 2004-05 year study. Concentration decreases of these two species were recorded in 2012 compared to those in 2011.

Nitrate concentrations had similar annual trends at MK and TW. Nitrate kept increasing during the first three one-year studies and decreased in the 4th year study. In the 5th year study, the nitrate concentrations further decreased by 46.1 and 43.5% at MK and TW sites, respectively. At YL site, on the other hand, nitrate decreased from the 2nd year study to the 3rd year study, increased again in the 4th year study, and then decreased by 44.6% in the 5th study.

OC concentrations decreased consistently across the MK, TW, and YL sites in the 5th year study by 12.8%, 16.0%, and 18.1%, respectively, compared to the 4th year study. Meanwhile, the EC concentrations exhibited different trends. EC increased by 8.5% at MK and decreased by 15.2 and 21.7% at TW and YL sites, respectively.

Crustal materials (Al, Si, Ca, and Fe) generally showed a decreasing trend in the 2001 - 2009 period but then kept increasing ever since. After a quite significant increase in 2011, the concentrations of the geological material further increased by 11.2, 5.0 and 3.0% at MK, TW and YL sites, respectively in the year of 2012.

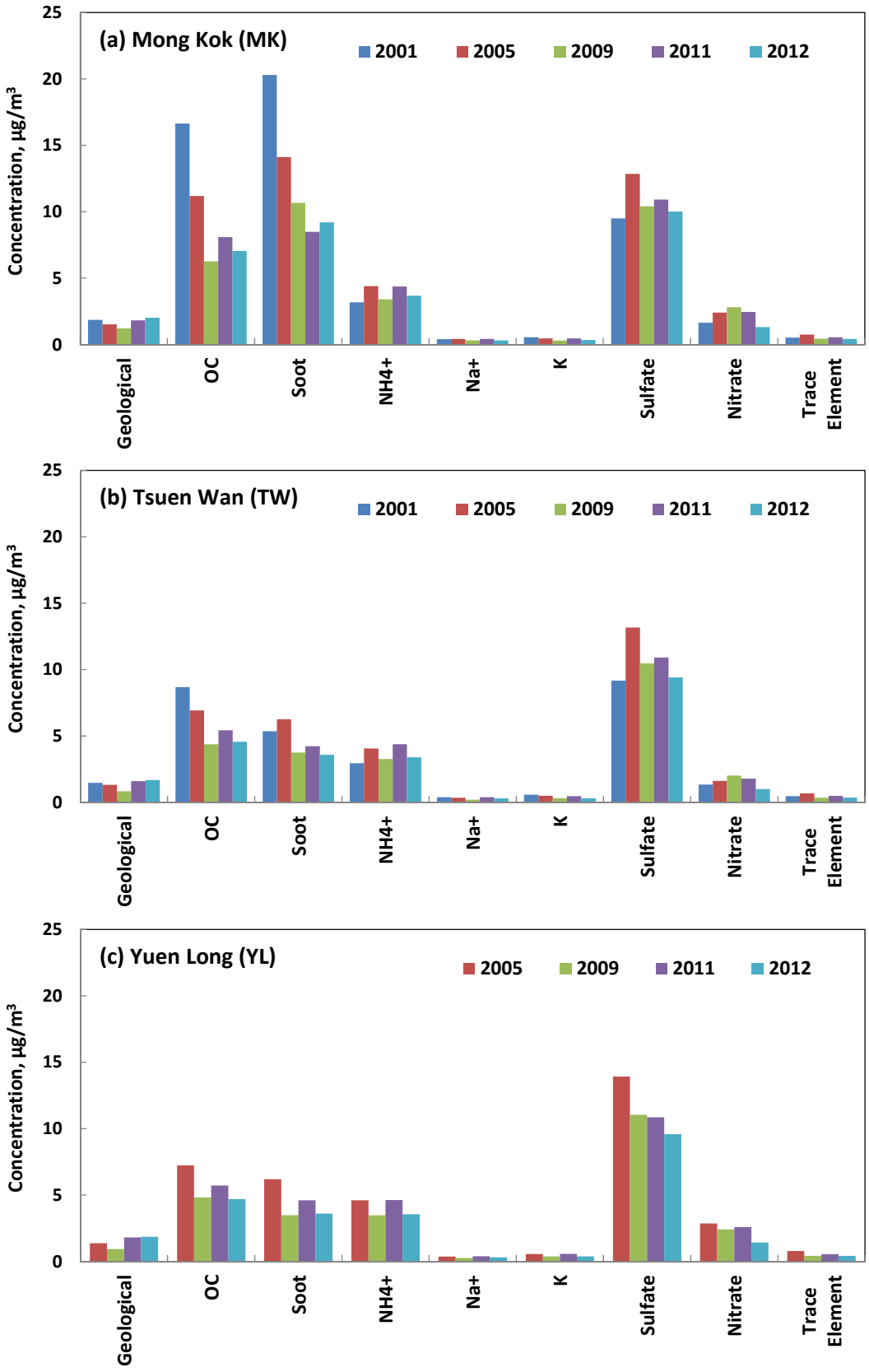

Figure 16. Annual trend of major components of $PM_{2.5}$ samples collected at (a) MK, (b) TW, and (c) YL.

5. Summary

During the period from February, 2012 to December 31, 2012, a $PM_{2.5}$ sampling campaign was conducted every sixth day in Hong Kong at six sites representing air quality at roadside, urban, new town, and suburban areas. A total of 330 samples (55 samples for each site) were collected from the Mong Kok (MK), Central Western (CW), Clear Water Bay (WB), Tung Chung (TC), Tsuen Wan (TW), and Yuen Long (YL) sites. The valid data percentage is approx. 93%. The highest annual average $PM_{2.5}$ mass of about 38.9 $\mu g/m^3$ was measured at the roadside MK site. The lowest annual average $PM_{2.5}$ mass of about 25.5 $\mu g/m^3$ was found at the suburban WB site. The $PM_{2.5}$ concentrations at 5 out of the 6 sampling sites were within the newly proposed HK AQO annual $PM_{2.5}$ standard of 35 $\mu g/m^3$.

Two levels of validation were performed on the complete data set. Reconstructed mass and measured mass were highly correlated with correlation coefficients (R^2) ranging from 0.97 to 0.98. It further supports the validity of both gravimetric analysis and chemical measurements. The reconstructed mass averagely explains approx. 90% of the measured $PM_{2.5}$ mass.

Sulfate is the most abundant component in the $PM_{2.5}$ across the five sites (25.7 - 36.6%). Nitrate concentrations as measured in the quartz filters were much lower than those of sulfate, contributing approx. 2.0 - 4.8% to the total mass at all sites. Ammonium was reasonably balanced by sulfate and nitrate and it was suggested to exist dominantly as ammonium sulfate over the Hong Kong region in the year of 2012. Both OC and EC concentrations were consistently higher at MK than at the other five sites. The lowest average EC value was found at WB site, which is in a relatively clean area with little commercial development.

Monthly average $PM_{2.5}$ concentration and chemical composition for each of the individual site are shown in Figure 17 in order to examine the seasonal trends of the different air pollutants. The results suggest that the entire Hong Kong region experienced higher $PM_{2.5}$ concentrations in winter months (Jan, Feb, Nov, and Dec) while the spring and summer months (Apr - Aug) usually have lower PM levels. The meteorological conditions play an important role in this situation. In winter time, the northerly and northeasterly winds prevail, bringing in air pollutants from mainland China. During summer, wind directions change to southerly and southeasterly and the clean marine air helps to dilute air pollutants in Hong Kong.

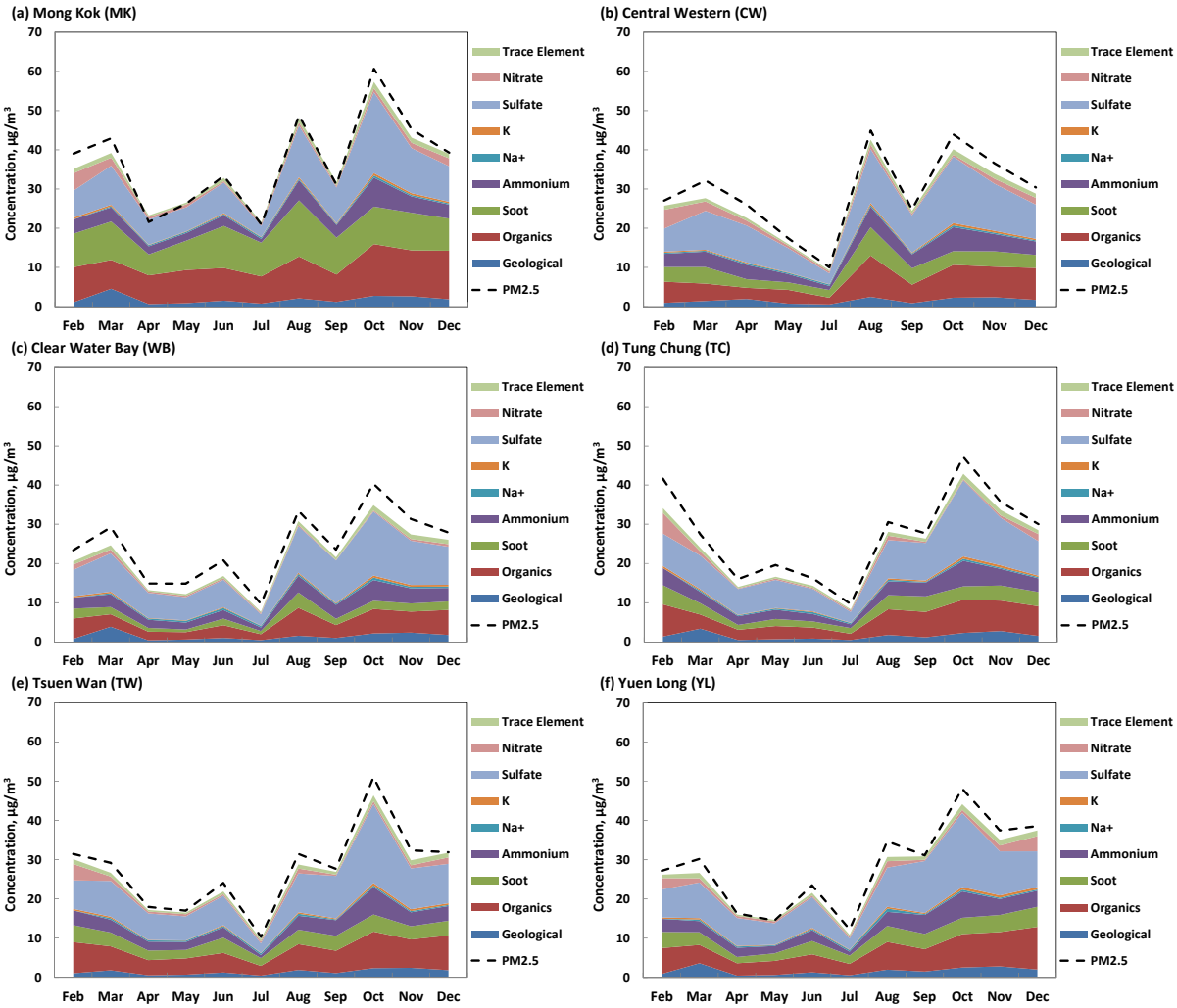

Figure 17. Monthly average of $PM_{2.5}$ mass concentrations and chemical compositions for (a) MK, (b) CW, (c) WB, (d) TC, (e) TW, and (f) YL during 2012 PM study. Note: no valid data is available for CW AQMS in June 2012.

The annual average $PM_{2.5}$ concentrations at the six sampling sites all exhibited a decrease in 2012 compared to those in 2011. Seen from the evaluation of variations of major PM components at different sites, the decrease of the PM concentrations were mainly attributable to the decreasing levels of sulfate, ammonium, nitrate and OC.

EC concentrations were significantly higher at MK site than at the other five sites and showed little seasonal variations. This is consistent with the characteristics of the roadside sampling site where local sources (e.g. vehicle exhausts) made dominant contributions to the observed EC level. The general decreasing trend of EC levels at MK from 2001 to 2012 indicates control measures of vehicular emissions are effective over the years.

The geological material concentrations have been increasing since 2008, suggesting the influence of dust storms coming from the mainland China especially during spring season (March and April).

References

Birch, M. E. and R. A. Cary (1996), Elemental carbon-based method for monitoring occupational exposures to particulate diesel exhaust, *Aerosol Sci. Technol.*, 25, 221-241.

Chen, L. -W. A., J. C. Chow, J. G. Watson, H. Moosmüller, and W. P. Arnott (2004), Modeling reflectance and transmittance of quartz-fiber filter samples containing elemental carbon particles: Implications for thermal/optical analysis, *J. Aerosol Sci.*, 35, 765-780.

Chow, J. C., J. G. Watson, L. C. Pritchett, W. R. Pierson, C. A. Frazier, and R. G. Purcell (1993), The DRI thermal/optical reflectance carbon analysis system: description, evaluation and applications in U. S. air quality studies, *Atmos. Environ.*, 27A, 1185-1201.

Chow, J. C., J. G. Watson, L. -W. A. Chen, W. P. Arnott, H. Moosmüller, and K. K. Fung (2004), Equivalence of elemental carbon by Thermal/Optical Reflectance and Transmittance with different temperature protocols, *Environ. Sci. Technol.*, 38, 4414-4422.

Chow J. C., J. G. Watson, L. -W. A. Chen, M. C. O. Chang, N. F. Robinson, D. Trimble, and S. D. Kohl (2007), The IMPROVE_A temperature protocol for thermal/optical carbon analysis: maintaining consistency with a long-term database, *J. Air Waste Manage. Assoc.*, 57, 1014-1023.

Chow J. C., J. G. Watson, Kohl, S. D., Gonzi, M. P., L. -W. A. Chen (2002), Measurements and Validation for the Twelve Month Particulate Matter Study in Hong Kong, report prepared for Hong Kong Environmental Protection Department. Available at the HKEPD official website: http://www.epd.gov.hk/epd/english/environmentinhk/air/studyrpts/files/final_version_hkepdfinalreport_rev12-12-02.pdf.

Chow J. C., J. G. Watson, Kohl, S. D., Voepel, H. E., L. -W. A. Chen (2006), Measurements and Validation for the Twelve Month Particulate Matter Study in Hong Kong, report prepared for Hong Kong Environmental Protection Department. Available at the HKEPD official website: http://www.epd.gov.hk/epd/english/environmentinhk/air/studyrpts/files/HKEPDFinalReportRev_V8.pdf.

Chow J. C., J. G. Watson, Kohl, S. D., L. -W. A. Chen (2010), Measurements and validation of the 2008/2009 particulate matter study in Hong Kong, report prepared for Hong Kong Environmental Protection Department. Available at the HKEPD official website: http://www.epd.gov.hk/epd/english/environmentinhk/air/studyrpts/files/HKEPDFinalReportRev_11-29-10_v2.pdf.

Subramanian, R., A. Y. Khlystov, and A. L. Robinson (2006), Effect of peak inert-mode temperature on elemental carbon measured using thermal-optical analysis, *Aerosol Sci. Technol.*, 40, 763-780.

Watson, J. G., J. C. Chow, and C. A. Frazier (1999), X-ray fluorescence analysis of ambient air samples, *Elemental Analysis of Airborne Particles, Vol 1*, by S. Landsberger and M. Creatchman, Eds. Gordon and Breach Science, Amsterdam, 67-96.

Yu, J. Z., X. H. H. Huang, and W. M. Ng (2012), Final report for provision of service for fine particulate matter ($PM_{2.5}$) sample chemical analysis, prepared for Hong Kong Environmental Protection Department.